2019 2nd Season Stock Assessment

Falkland calamari

(Doryteuthis gahi)

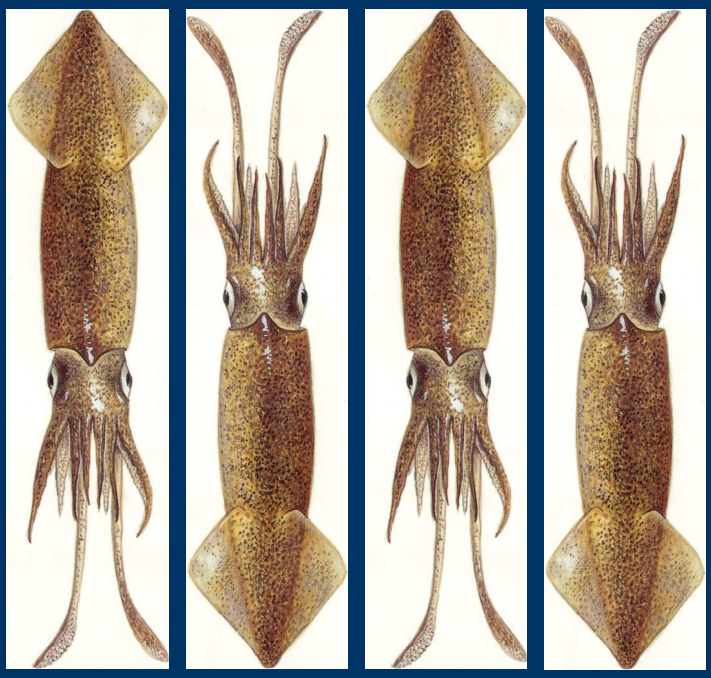

S2 - 2019 - LOL

Andreas Winter

Natural Resources - Fisheries
Falkland Islands Government
Stanley, Falkland Islands

November 2019

Index

Summary

1) The 2019 second season *Doryteuthis gahi* fishery (X license) was open from July 29th, and closed by emergency order for stock conservation on September 9th. 635 vessel-days were fished over the course of the 43 season days.
2) Six fishing mortalities of South American fur seals and one mortality of a Southern sea lion were recorded during the season. The use of Seal Exclusion Devices was mandated throughout the Loligo Box starting on July 30th, following two early mortalities.
3) 24,748 tonnes of *D. gahi* catch were reported in the X-license fishery; of which 48.5% in the first 9 days, and giving a season average CPUE of 39.0 t vessel-day^{-1}. During the season 14.0% of *D. gahi* catch and 26.7% of fishing effort were taken north of 52º S; 86.0% of *D. gahi* catch and 73.3% of fishing effort were taken south of 52º S.
4) In the north sub-area, one depletion period / immigration was inferred to have started on August 9th, the first day of fishing in the north. In the south sub-area, three depletion periods were inferred to have started on July 29th (start of the season), August 8th, and September 5th. The second depletion on August 8th was inferred as a net emigration (negative immigration) of squid, following a day of severe weather.
5) The balance of the season held that more squid were lost through emigration or dispersal than arrived through in-season immigration. In the north, estimated net emigration was 619 t (95% confidence interval -7 to 1099 t), most of it concentrated in a few days close to the severe weather day in the south on August 7th. In the south, estimated net emigration was 6394 t (95% confidence interval 1501 to 14,078 tonnes); almost entirely attributed to the 2nd depletion start on August 8th.
6) The estimate of *D. gahi* escapement biomass remaining at the end of second season 2019 depended on the assumption of how much of the dispersed/emigrated squid ultimately re-joined the spawning stock. The two estimate limit points were:
   Considering in-zone biomass only at the end of the season, escapement was a maximum likelihood of 9,505 tonnes, with a 95% confidence interval of 6,518 to 27,963 t. The risk of this escapement being less than 10,000 tonnes was 36.6%.
   Considering in-zone biomass plus surviving dispersed biomass at the end of the season, escapement was a maximum likelihood of 14,757 tonnes with a 95% confidence interval of 8,350 to 40,416 t. The risk of this escapement being less than 10,000 tonnes was 6.6%.

Introduction

The second season of the 2019 *Doryteuthis gahi* fishery (Falkland calamari – colloquially *Loligo*) opened on July 29th. During the season 4 flex days were requested for mechanical repairs by various vessels, one vessel delayed entry by 2 days due to repairs in route, and one vessel fished on a licence substitution 2 days for another vessel being repaired. Twenty-one flex days were requested for in-season bad weather, of which 14 on August 7th[a], 3 on August 8th, 3 on August 10th, and 1 on September 3rd (Figure 1). The season was closed by emergency order at 23:59 on September 9th. All flex days were consequently voided.

As in previous seasons since 2018, X-licensed vessels were required to embark an observer tasked (at minimum) to monitor the presence and incidental capture of pinnipeds. The occurrence of two pinniped mortalities resulted in mandatory use of Seal Exclusion Devices (SEDs) in the entire Loligo Box fishing zone starting from 00:01 on July 30th; that is one day after the opening of the season.

[a] In fact, no vessels fished on August 7th, but two vessels opted not to request a bad-weather day.

Total reported *D. gahi* catch under second season X license was 3,469 north + 21,279 south = 24,748 tonnes (Table 1), corresponding to an overall average CPUE of 24748 / 635 = 39.0 tonnes vessel-day^{-1}. The average CPUE was actually the highest for a second season since at least 2004 (Table 1), presenting an unusual scenario for a season that was closed by emergency order.

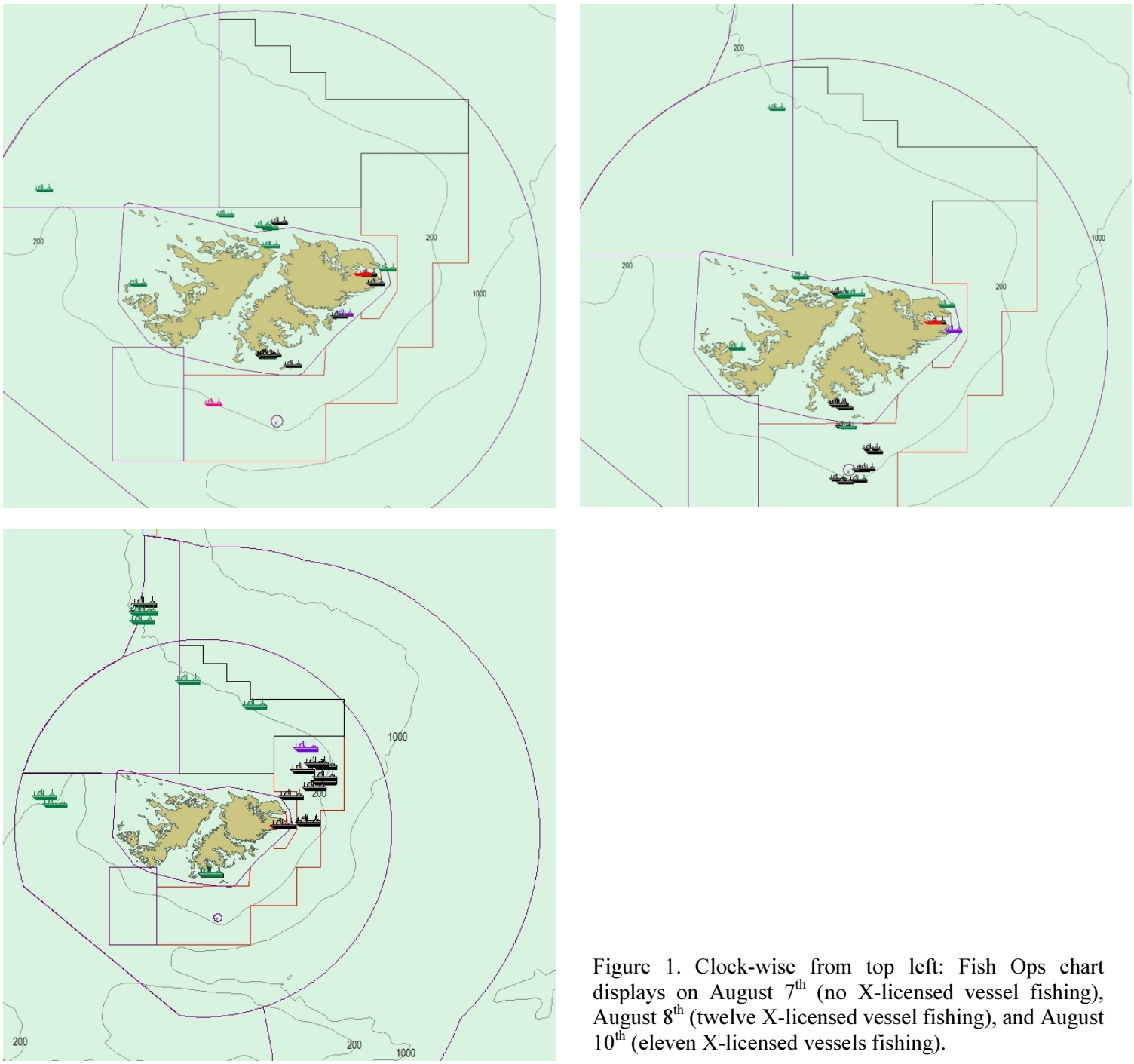

Figure 1. Clock-wise from top left: Fish Ops chart displays on August 7th (no X-licensed vessel fishing), August 8th (twelve X-licensed vessel fishing), and August 10th (eleven X-licensed vessels fishing).

Assessment of the Falkland Islands *D. gahi* stock was conducted with depletion time-series models as in previous seasons (Agnew et al. 1998, Roa-Ureta and Arkhipkin 2007; Arkhipkin et al. 2008), and in other squid fisheries (Royer et al. 2002, Young et al. 2004,

Chen et al. 2008, Morales-Bojórquez et al. 2008, Keller et al. 2015, Medellín-Ortiz et al. 2016). Because *D. gahi* has an annual life cycle (Patterson 1988, Arkhipkin 1993), stock cannot be derived from a standing biomass carried over from prior years (Rosenberg et al. 1990, Pierce and Guerra 1994). The depletion model instead calculates an estimate of population abundance over time by evaluating what levels of abundance and catchability must be extant to sustain the observed rate of catch. Depletion modelling of the *D. gahi* target fishery is used both in-season and for the post-season summary, with the objective of maintaining an escapement biomass of 10,000 tonnes *D. gahi* at the end of each season as a conservation threshold (Agnew et al. 2002, Barton 2002).

Table 1. *D. gahi* season comparisons since 2004, when catch management was assumed by the FIFD. Days: total number of calendar days open to licensed *D. gahi* fishing including (since 1st season 2013) optional extension days; V-Days: aggregate number of licensed *D. gahi* fishing days reported by all vessels for the season. Entries in italics are seasons closed by emergency order.

	Season 1			Season 2		
	Catch (t)	Days	V-Days	Catch (t)	Days	V-Days
2004	7,152	46	625	17,559	78	1271
2005	24,605	45	576	29,659	78	1210
2006	19,056	50	704	*23,238*	*53*	*883*
2007	17,229	50	680	*24,171*	*63*	*1063*
2008	24,752	51	780	26,996	78	1189
2009	12,764	50	773	*17,836*	*59*	*923*
2010	28,754	50	765	36,993	78	1169
2011	15,271	50	771	*18,725*	*70*	*1099*
2012	34,767	51	770	35,026	78	1095
2013	19,908	53	782	19,614	78	1195
2014	28,119	59	872	19,630	71	1099
2015	*19,383**	*57**	*871**	*10,190*	*42*	*665*
2016	22,616	68	1020	23,089	68	1004
2017	39,433	68	999†	24,101	69	1002‡
2018	43,085	69	975	35,828	68	977
2019	55,586	68	953	*24,748*	*43*	*635*

* Does not include C-license catch or effort after the C-license target for that season was switched from *D. gahi* to *Illex*.
† Includes two vessel-days of experimental fishing for juvenile toothfish.
‡ Includes one vessel-day of experimental fishing for juvenile toothfish.

Methods

The depletion model formulated for the Falklands *D. gahi* stock is based on the equivalence:

$$C_{day} = q \times E_{day} \times N_{day} \times e^{-M/2} \quad \textbf{(1)}$$

where q is the catchability coefficient, M is the natural mortality rate (considered constant at 0.0133 day^{-1}; Roa-Ureta and Arkhipkin 2007), and C_{day}, E_{day}, N_{day} are catch (numbers of squid), fishing effort (numbers of vessels), and abundance (numbers of squid) per day. In its basic form (DeLury 1947) the depletion model assumes a closed population in a fixed area for the duration of the assessment. However, the assumption of a closed population is imperfectly met in the Falkland Islands fishery, where stock analyses have often shown that

D. gahi groups arrive in successive waves after the start of the season (Roa-Ureta 2012; Winter and Arkhipkin 2015). Arrivals of successive groups are inferred from discontinuities in the catch data. Fishing on a single, closed cohort would be expected to yield gradually decreasing CPUE, but gradually increasing average individual sizes, as the squid grow. When instead these data change suddenly, or in contrast to expectation, the immigration of a new group to the population is indicated (Winter and Arkhipkin 2015).

In the event of a new group arrival, the depletion calculation must be modified to account for this influx. This is done using a simultaneous algorithm that adds new arrivals on top of the stock previously present, and posits a common catchability coefficient for the entire depletion time-series. If two depletions are included in the same model (i.e., the stock present from the start plus a new group arrival), then:

$$C_{day} = q \times E_{day} \times (N1_{day} + (N2_{day} \times i2|_0^1)) \times e^{-M/2} \quad \textbf{(2)}$$

where i2 is a dummy variable taking the values 0 or 1 if 'day' is before or after the start day of the second depletion. For more than two depletions, $N3_{day}$, i3, $N4_{day}$, i4, etc., would be included following the same pattern.

In previous seasons since second season 2017, the depletion equation **(2)** was further modified to differentiate between catches taken with or without SEDs installed in the trawl nets. In this season, with the survey run without SEDs (Goyot et al. 2019) but SEDs then ordered just one day after the start of commercial fishing, differentiation would be impossible to model effectively. However, an analysis computed with last season's data found that daily biomass estimation did not change significantly between the implementation or not of SED differentiation (Winter 2019). An SED factor was therefore not included and all catch efficiencies were considered part of the fleet's overall range of variation.

The season depletion likelihood function was calculated as the difference between actual catch numbers reported and catch numbers predicted from the model (Equation **2**), statistically corrected by a factor relating to the number of days of the depletion period (Roa-Ureta 2012):

$$((n\text{Days} - 2)/2) \times \log\left(\sum_{days}\left(\log(\text{predicted}\,C_{day}) - \log(\text{actual}\,C_{day})\right)^2\right) \quad \textbf{(3)}$$

The stock assessment was set in a Bayesian framework (Punt and Hilborn 1997), whereby results of the season depletion model are conditioned by prior information on the stock; in this case the information from the pre-season survey.

The likelihood function of prior information was calculated as the normal distribution of the difference between catchability (q) derived from the survey abundance estimate, and catchability derived from the season depletion model. Applying this difference requires both the survey and the season to be fishing the same stock with the same gear. Catchability, rather than abundance N, is used for calculating prior likelihood because catchability informs the entire season time series; whereas N from the survey only informs the first in-season depletion period – subsequent immigrations and depletions are independent of the abundance that was present during the survey. Thus, the prior likelihood function was:

$$\frac{1}{\sqrt{2\pi \cdot SD_{q\,prior}{}^2}} \times \exp\left(-\frac{\left(q_{model} - q_{prior}\right)^2}{2 \cdot SD_{q\,prior}{}^2}\right) \quad \textbf{(4)}$$

where the standard deviation of catchability prior ($SD_{q\ prior}$) was calculated from the Euclidean sum of the survey prior estimate uncertainty, the variability in catches on the season start date, and the uncertainty in the natural mortality M estimate over the number of days mortality discounting (Appendix: Equations **A5-N**, **A5-S**).

Bayesian optimization of the depletion was calculated by jointly minimizing Equations **3** and **4**, using the Nelder-Mead algorithm in R programming package 'optimx' (Nash and Varadhan 2011). Relative weights in the joint optimization were assigned to Equations **3** and **4** as the converse of their coefficients of variation (CV), i.e., the CV of the prior became the weight of the depletion model and the CV of the depletion model became the weight of the prior. Calculations of the depletion CVs are described in Equations **A8-N** and **A8-S**. Because a complex model with multiple depletions may converge on a local minimum rather than global minimum, the optimization was stabilized by running a feed-back loop that set the q and N parameter outputs of the Bayesian joint optimization back into the in-season-only minimization (Equation **3**), re-calculated this minimization and the CV resulting from it, then re-calculated the Bayesian joint optimization, and continued this process until both the in-season minimization and the joint optimization remained unchanged.

With actual C_{day}, E_{day} and M being fixed parameters, the optimization of Equation **2** using Equations **3** and **4** produces estimates of q and N1, N2, …, etc. Numbers of squid on the final day (or any other day) of a time series are then calculated as the numbers N of the depletion start days discounted for natural mortality during the intervening period, and subtracting cumulative catch also discounted for natural mortality (CNMD). Taking for example a two-depletion period:

$$\begin{aligned} N_{final\ day} &= N1_{start\ day\ 1} \times e^{-M\ (final\ day\ -\ start\ day\ 1)} \\ &+ N2_{start\ day\ 2} \times e^{-M\ (final\ day\ -\ start\ day\ 2)} \\ &- CNMD_{final\ day} \end{aligned} \quad \textbf{(5)}$$

where

$$CNMD_{day\ 1} = 0$$

$$CNMD_{day\ x} = CNMD_{day\ x-1} \times e^{-M} + C_{day\ x-1} \times e^{-M/2} \quad \textbf{(6)}$$

$N_{final\ day}$ is then multiplied by the average individual weight of squid on the final day to give biomass. Daily average individual weight is obtained from length / weight conversion of mantle lengths measured in-season by observers, and also derived from in-season commercial data as the proportion of product weight that vessels reported per market size category. Observer mantle lengths are scientifically accurate, but restricted to 1-2 vessels at any one time that may or may not be representative of the entire fleet, and not available every day. Commercially proportioned mantle lengths are relatively less accurate, but cover the entire fishing fleet every day. Therefore, both sources of data are used (see Appendix – *Doryteuthis gahi* individual weights).

Distributions of the likelihood estimates from joint optimization (i.e., measures of their statistical uncertainty) were computed using a Markov Chain Monte Carlo (MCMC) (Gamerman and Lopes 2006), a method that is commonly employed for fisheries assessments (Magnusson et al. 2013). MCMC is an iterative process which generates random stepwise changes to the proposed outcome of a model (in this case, the q and N of *D. gahi* squid) and at each step, accepts or nullifies the change with a probability equivalent to how well the change fits the model parameters compared to the previous step. The resulting sequence of accepted or nullified changes (i.e., the 'chain') approximates the likelihood distribution of the model outcome. The MCMC of the depletion models were run for 200,000 iterations; the first

1000 iterations were discarded as burn-in sections (initial phases over which the algorithm stabilizes); and the chains were thinned by a factor equivalent to the maximum of either 5 or the inverse of the acceptance rate (e.g., if the acceptance rate was 12.5%, then every 8th (0.125^{-1}) iteration was retained) to reduce serial correlation. For each model three chains were run; one chain initiated with the parameter values obtained from the joint optimization of Equations **3** and **4**, one chain initiated with these parameters ×2, and one chain initiated with these parameters ×¼. Convergence of the three chains was accepted if the variance among chains was less than 10% higher than the variance within chains (Brooks and Gelman 1998). When convergence was satisfied the three chains were combined as one final set. Equations **5**, **6**, and the multiplication by average individual weight were applied to the CNMD and each iteration of N values in the final set, and the biomass outcomes from these calculations represent the distribution of the estimate. The peaks of the MCMC histograms were compared to the empirical optimizations of the N values.

Depletion models and likelihood distributions were calculated separately for north and south sub-areas of the Loligo Box fishing zone, as *D. gahi* sub-stocks emigrate from different spawning grounds and remain to an extent segregated (Arkhipkin and Middleton 2002). Total escapement biomass is then defined as the aggregate biomass of *D. gahi* on the last day of the season for north and south sub-areas combined. North and south biomasses are not assumed to be uncorrelated however (Shaw et al. 2004), and therefore north and south likelihood distributions were added semi-randomly in proportion to the strength of their day-to-day correlation (see Winter 2014, for the semi-randomization algorithm).

Stock assessment

Data

The north sub-area was fished on 30 of the 43 season-days, for 14.0% of the total catch (3469.3 t *D. gahi*) and 26.7% of the effort (169.7 vessel-days) (Figure 2). On eight days effort was higher in the north than in the south (Figure 3). The south sub-area was fished on 41 of the 43 season-days, for 86.0% of total catch (21278.8 t *D. gahi*) and 73.3% of effort (465.3 vessel-days). 56.4% of south catch (and thereby 48.5% of total catch) was taken before August 7th; that is within the first 9 days of the season.

635 vessel-days were fished during the season (Table 1), with a median of 15 vessels per day (mean 14.77). Vessels reported daily catch totals to the FIFD and electronic logbook data that included trawl times, positions, depths, and product weight by market size categories. With the shortened season just two FIG fishery observers were deployed for a total of 37 sampling days[b] (Kairua 2019, Tutjavi 2019). Throughout the 43 days of the season, 6 days had no FIG fishery observer covering, 33 days had one FIG fishery observer covering, and 4 days had two FIG fishery observers covering. Except for seabird days FIG fishery observers were tasked with sampling 200 *D. gahi* at two stations; reporting their maturity stages, sex, and lengths to 0.5 cm. Contract marine mammal monitors were tasked with measuring 200 unsexed lengths of *D. gahi* per day. The length-weight relationship for converting observer and commercially proportioned lengths was combined from 2nd pre-season and season length-weight data of both 2018 and 2019, as 2019 data became available progressively with on-going observer coverage. Final parameterization of the length-weight relationship included 2220 measures from 2018 and 2999 measures from 2019, giving:

$$\text{weight (kg)} = 0.16358 \times \text{length (cm)}^{2.20828} / 1000 \quad \textbf{(7)}$$

[b] Not counting seabird days (every fourth day).

with a coefficient of determination R^2 = 90.4%.

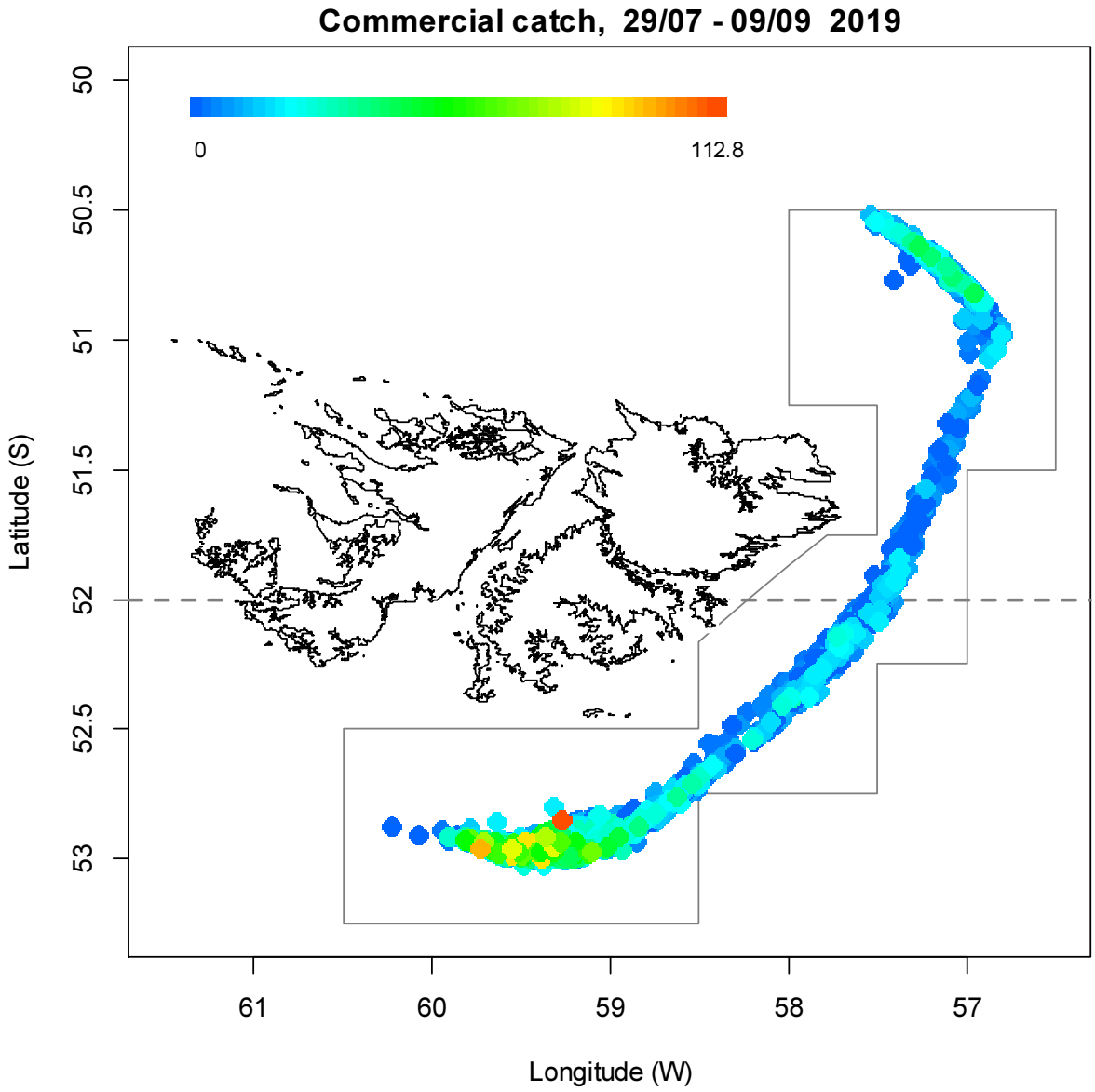

Figure 2. Spatial distribution of *D. gahi* 2nd-season trawls, colour-scaled to catch weight (maximum = 112.8 tonnes). 1881 trawl catches were taken during the season. The 'Loligo Box' fishing zone, as well as the 52 ºS parallel delineating the boundary between north and south assessment sub-areas, are shown in grey.

Figure 3 [next page]. Daily total *D. gahi* catch and effort distribution by assessment sub-area north (green) and south (purple) of the 52º S parallel during 2nd season 2019. The season was open from July 29th (chronological day 210) to September 9th (chronological day 252). Orange under-shading delineates the mandatory use of SEDs north and south. Yellow under-shading delineates emergency closure of the fishery after September 9th through the scheduled season end on September 30th (chronological day 273). As many as 12 vessels fished per day north; as many as 16 vessels fished per day south. As much as 412 tonnes *D. gahi* was caught per day north; as much as 1459 tonnes *D. gahi* was caught per day south.

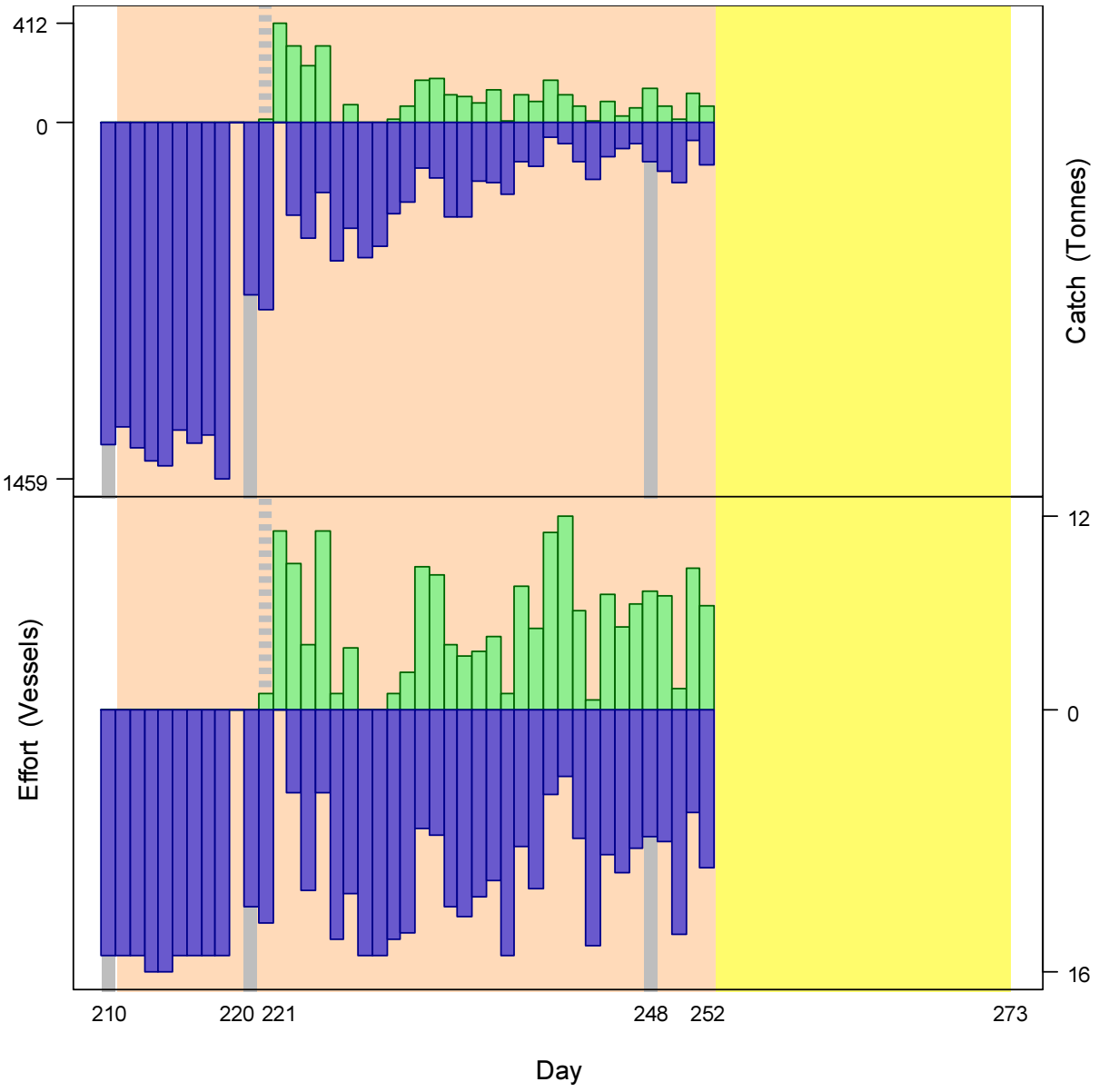

Group arrivals / depletion criteria

Start days of depletions - following arrivals of new *D. gahi* groups - were judged primarily by daily changes in CPUE, with additional information from sex proportions, maturity, and average individual squid sizes. CPUE was calculated as metric tonnes of *D. gahi* caught per vessel per day. Days were used rather than trawl hours as the basic unit of effort. Commercial vessels do not trawl standardized duration hours, but rather durations that best suit their daily processing requirements. An effort index of days is therefore more consistent.

One day in the north and three days in the south were identified that represented the onset of separate depletion starts throughout the season.

- The first depletion north was set on day 221 (August 9th), the first day that fishing was taken in the north by a single vessel. While CPUE was not yet high (Figure 5), the subsequent trends of increasing average weights (Figures 6A and 6B), increasing maturity

(Figure 6D), and level female proportion (Figure 6C) indicate that the biomass was present on day 221.

- The first depletion south was set on day 210 (July 29th), the first day of the season with all 15 vessels that started the season fishing south. CPUE stayed at a consistent high level for the next 8 days (Figure 5).
- The second depletion south was set on day 220 (August 8th), the day after fishing was stopped completely due to bad weather (Figure 1). CPUE from that day on remained categorically lower than before August 7th (Figure 5), effectively marking a negative immigration[c] of squid that were assumed to have dispersed irrecoverably out of the fishing zone.
- The third depletion south was identified on day 248 (September 5th) with the highest CPUE in 10 days, followed by higher CPUE the next day (Figure 5). Average individual weight was at a local minimum (Figures 6A and 6B).

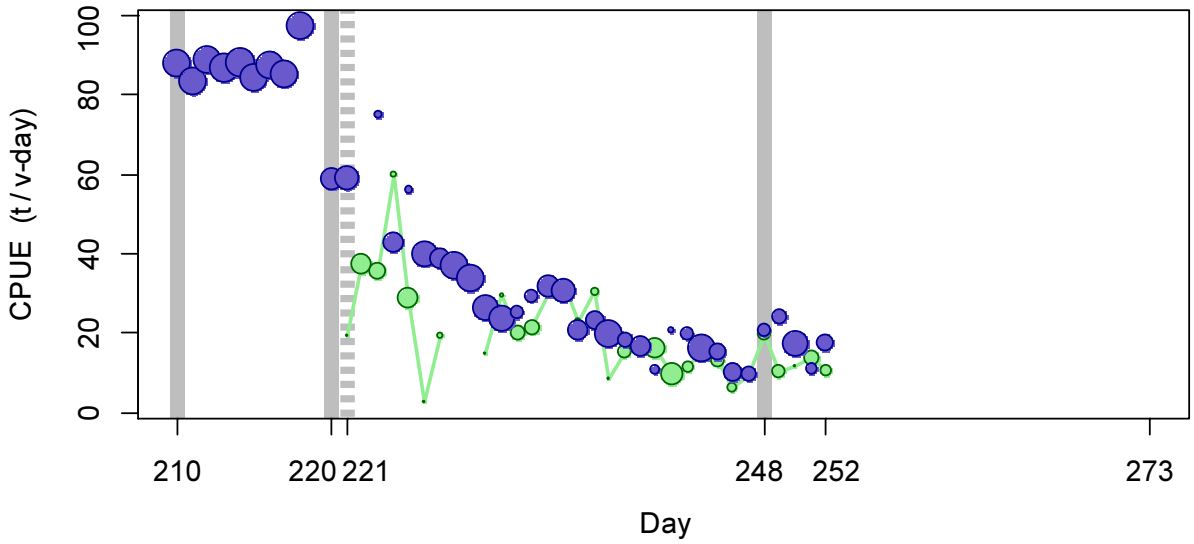

Figure 5. CPUE in metric tonnes per vessel per day, by assessment sub-area north (green) and south (purple) of 52° S latitude. Circle sizes are proportioned to numbers of vessels fishing. Data from consecutive days are joined by line segments. Broken grey bars indicate the starts of in-season depletions north. Solid grey bars indicate the starts of in-season depletions south.

Figure 6 [next page]. A: Average individual *D. gahi* weights (kg) per day from commercial size categories. B: Average individual *D. gahi* weights (kg) by sex per day from observer sampling. C: Proportions of female *D. gahi* per day from observer sampling. D: Average maturity value by sex per day from observer sampling. In all graphs – Males: triangles, females: squares, unsexed: circles. North sub-area: green, south sub-area: purple. Data from consecutive days are joined by line segments. Broken grey bars indicate the starts of in-season depletions north. Solid grey bars indicate the starts of in-season depletions south.

[c] Negative immigration is computationally feasible, but required a modification for coding the algorithm. The optimization of Equation **2** is normally operated on values of N and q entered in log scale, which cannot be applied to negative values. The algorithm was therefore rewritten to enter N_2 (the second immigration/depletion start) in linear scale.

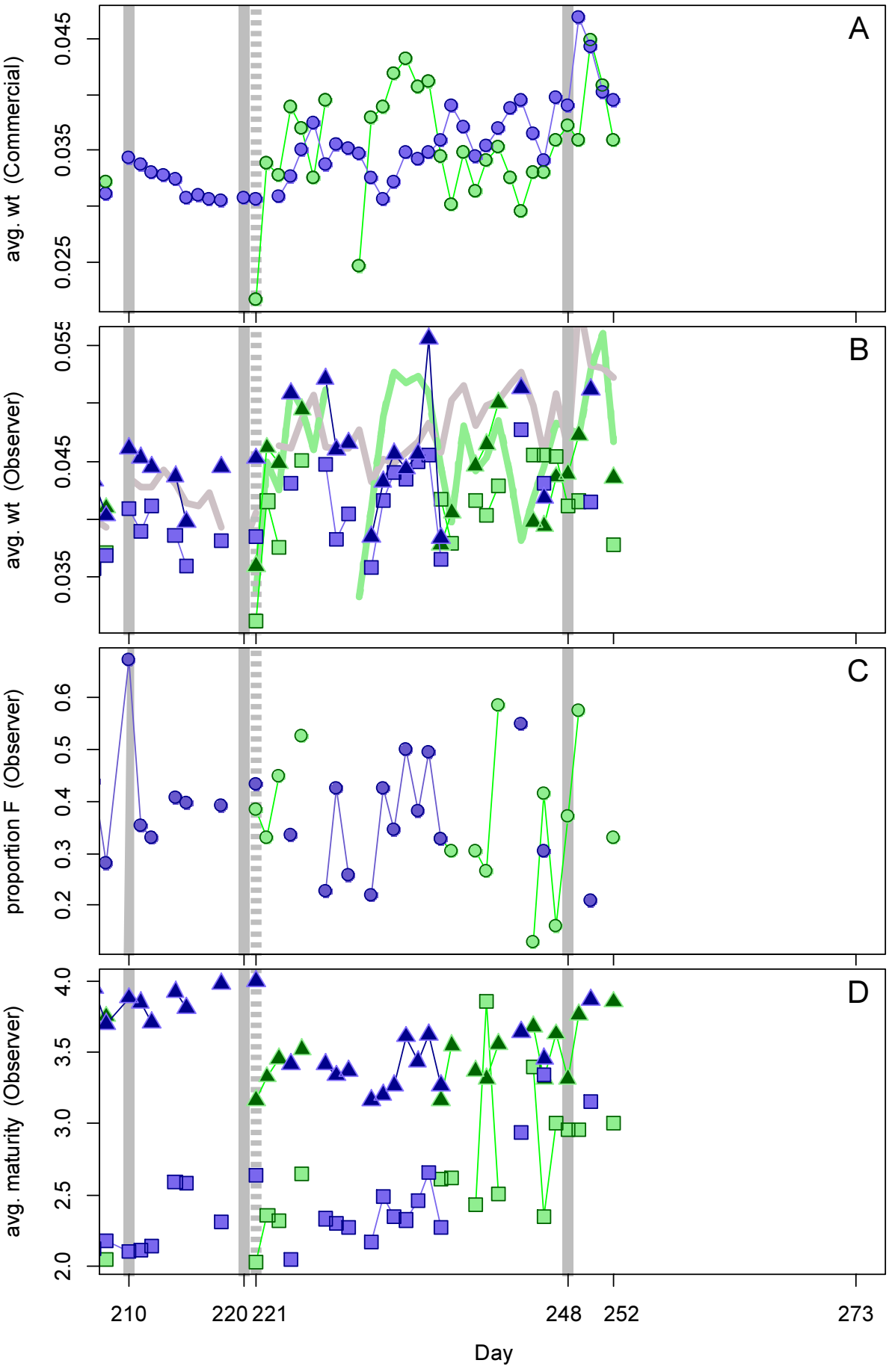
A
avg. wt (Commercial)
0.025
0.035
0.045
B
avg. wt (Observer)
0.035
0.045
0.055
C
proportion F (Observer)
0.2
0.3
0.4
0.5
0.6
D
avg. maturity (Observer)
2.0
2.5
3.0
3.5
4.0
210
220
221
248
252
273
Day

Depletion analyses

North

In the north sub-area, Bayesian optimization on catchability (q) resulted in a posterior (maximum likelihood $_{\text{Bayesian}}\ q_N = 2.541 \times 10^{-3}$ (Figure 6, left, and Equation **A9-N**) that was closer to the pre-season prior ($_{\text{prior}}\ q_N = 2.311 \times 10^{-3}$; Figure 6, left, and Equation **A4-N**) than the in-season depletion ($_{\text{depletion}}\ q_N = 3.323 \times 10^{-3}$; Figure 6, left, and Equation **A6-N**). Respective weights in the Bayesian optimization (converse of the CVs) were 1.030 for the in-season depletion (Equation **A5-N**) and 0.411 for the prior (Equation **A8-N**).

The MCMC distribution of the Bayesian posterior multiplied by the generalized additive model (GAM) fit of average individual squid weight (Figure A1-N) gave the likelihood distribution of *D. gahi* biomass on last day 252 (September 9th) shown in Figure 6-right, with maximum likelihood and 95% confidence interval of:

$$B_{N\ \text{day}\ 252} = 4{,}492\ \text{t} \sim 95\%\ \text{CI}\ [2{,}452 - 119{,}861]\ \text{t} \qquad \textbf{(8-N)}$$

At its highest point (one day after the start of fishing: day 222 – August 10th), model-estimated *D. gahi* biomass north was 9,833 t ~ 95% CI [7,093 – 30,477] t (Figure 7). Variability remained high throughout the time period, and it is not statistically conclusive that any change in average biomass occurred during the season by the rule that a straight line could be drawn through the plot (Figure 7) without intersecting the 95% confidence intervals (Swartzman et al. 1992).

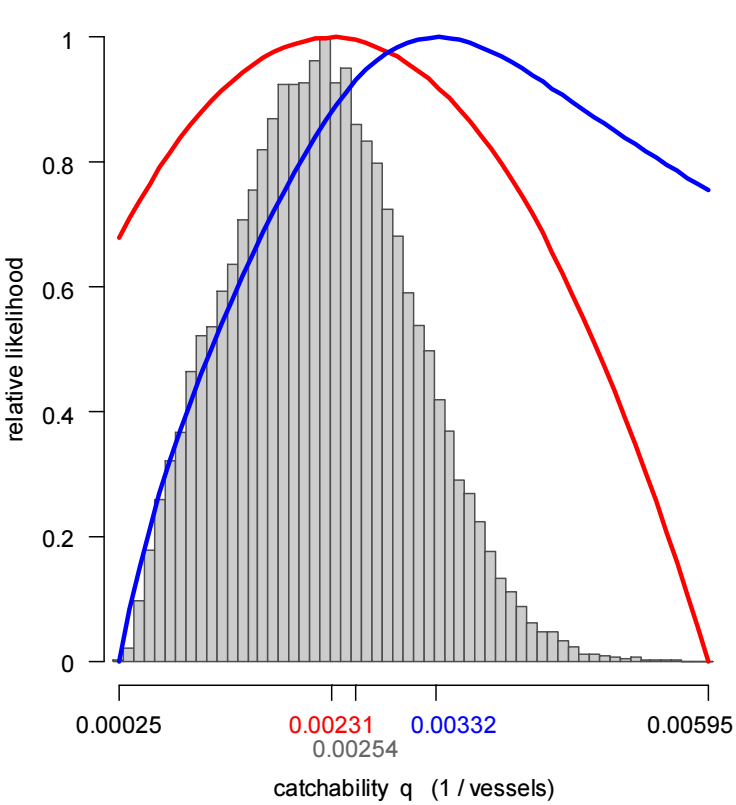

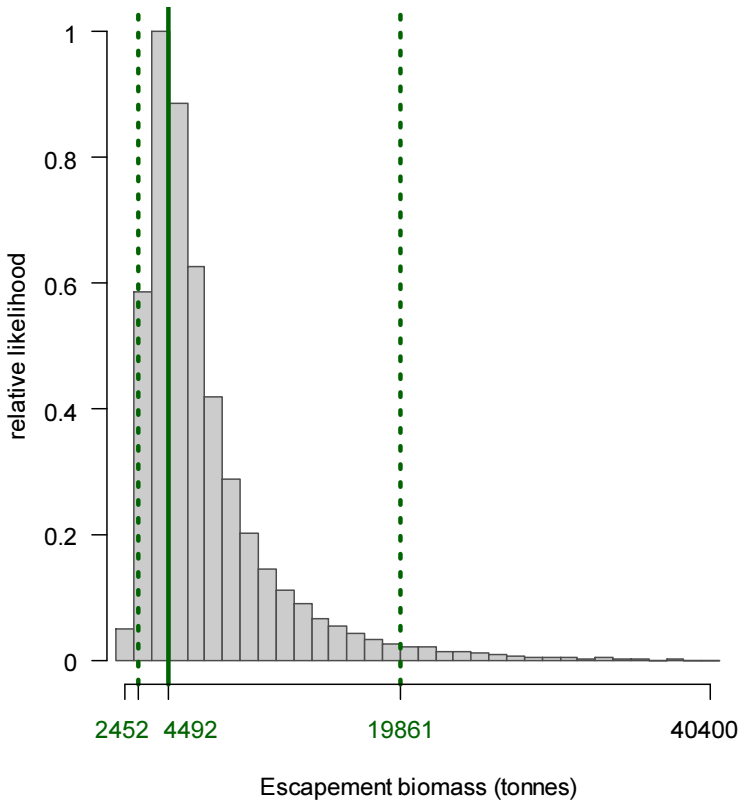

Figure 6 [previous page]. North sub-area. Left: Likelihood distributions for *D. gahi* catchability. Red line: prior model (pre-season survey data), blue line: in-season depletion model, grey bars: combined Bayesian model posterior. Right: Likelihood distribution (grey bars) of escapement biomass, from Bayesian posterior and average individual squid weight at the end of the season. Green lines: maximum likelihood and 95% confidence interval. Note the correspondence to Figure 7.

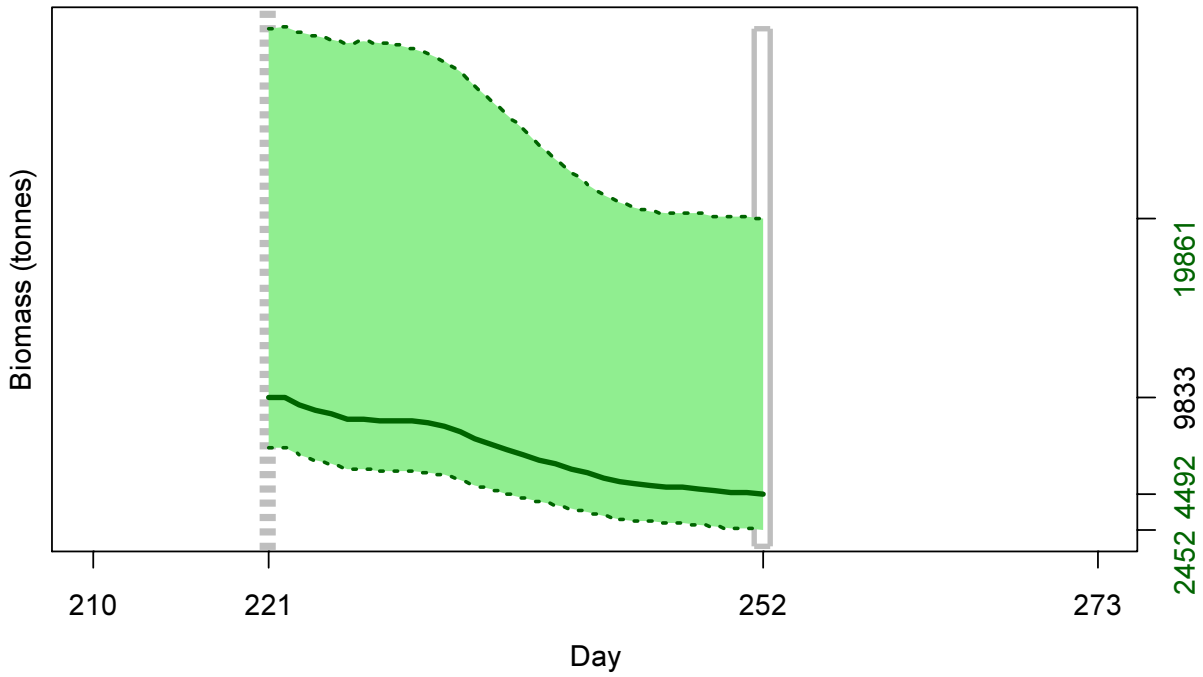

Figure 7. North sub-area. *D. gahi* biomass time series estimated from Bayesian posterior of the depletion model ± 95% confidence intervals. Broken grey bars indicate the start of in-season depletion north; day 221. Note that the biomass 'footprint' on day 252 (September 9th) corresponds to the right-side plot of Figure 6.

South

In the south sub-area, the unusual change of biomass in-season expectedly resulted in a Bayesian posterior optimization on catchability (q) ($_{\text{Bayesian}}\, q_S = 2.927 \times 10^{-3}$; Figure 8, left, and Equation **A9-S**) much closer to the pre-season prior ($_{\text{prior}}\, q_S = 2.753 \times 10^{-3}$; Figure 8, left, and Equation **A4-S**) than to the in-season depletion ($_{\text{depletion}}\, q_S = 4.315 \times 10^{-3}$; off the scale on Figure 8, left, and Equation **A6-S**). Respective weights in the Bayesian optimization (converse of the CVs) were 0.528 for the in-season depletion (Equation **A5-S**) and 1.387 for the prior (Equation **A8-S**).

The MCMC distribution of the Bayesian posterior multiplied by the GAM fit of average individual squid weight (Figure A1-S) gave the likelihood distribution of *D. gahi* biomass on day 252 (September 9th) shown in Figure 8-right, with maximum likelihood and 95% confidence interval of:

$$B_{S\ \text{day}\ 252} = 5{,}076\ \text{t} \sim 95\%\ \text{CI}\ [4{,}062 - 8{,}644]\ \text{t} \qquad \textbf{(8-S)}$$

On the first day of the season estimated *D. gahi* biomass south was 39,840 t ~ 95% CI [32,495 – 54,056] t (Figure 9); higher than but within range of the pre-season estimate of

32,364 t ~ 95% CI [28,509 – 50,709] t (Goyot et al. 2019). The in-zone biomass trend after day 220 was highly significantly lower than before day 220.

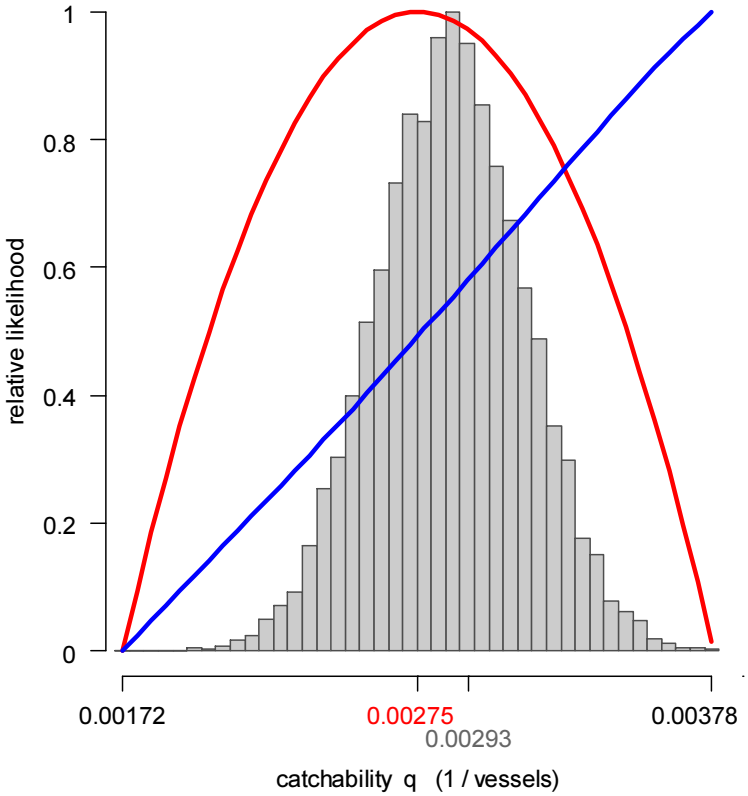

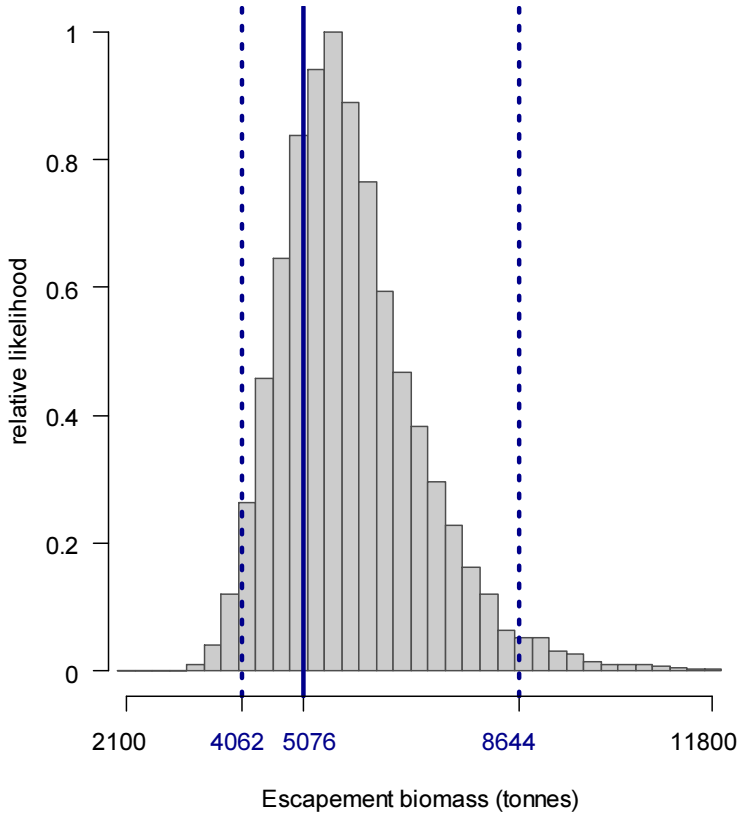

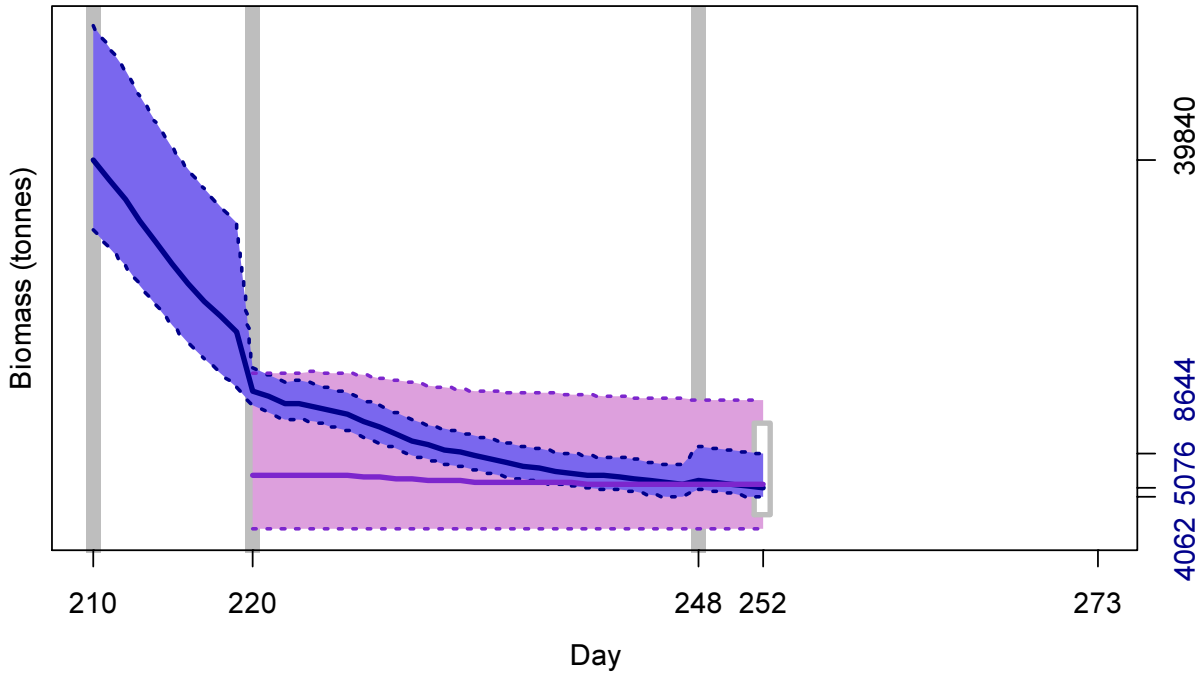

Figure 8 [previous page top]. South sub-area. Left: Likelihood distributions for *D. gahi* catchability. Red line: prior model (pre-season survey data), blue line: in-season depletion model, grey bars: combined Bayesian model posterior. Right: Likelihood distribution (grey bars) of escapement biomass, from Bayesian posterior and average individual squid weight at the end of the season. Blue lines: maximum likelihood and 95% confidence interval. Note correspondence to Figure 9.

Figure 9 [previous page bottom]. South sub-area. *D. gahi* biomass time series estimated from Bayesian posterior of the depletion model ± 95% confidence intervals (dark purple). Note that the biomass 'footprint' on day 252 (September 9th) corresponds to the right-side plot of Figure 8. *D. gahi* dispersed biomass estimated by extension from day 220 onward ± 95% confidence intervals (pale purple). Note that the dispersed biomass 'inherits' the wider confidence intervals of the time series prior to the second in-season depletion start. Grey bars indicate the start of in-season depletions south; days 210, 220, and 248.

Immigration

Doryteuthis gahi immigration during the season was inferred on each day by how many more squid were estimated present than the day before, minus the number caught and the number expected to have died naturally:

$$_{\text{Immigration}}N_{\text{day i}} = N_{\text{day i}} - (N_{\text{day i-1}} - C_{\text{day i-1}} - M_{\text{day i-1}})$$

where $N_{\text{day i-1}}$ are optimized in the depletion models, $C_{\text{day i-1}}$ calculated as in Equation **2**, and $M_{\text{day i-1}}$ is:

$$M_{\text{day i-1}} = (N_{\text{day i-1}} - C_{\text{day i-1}}) \times (1 - e^{-M})$$

Immigration biomass per day was then calculated as the immigration number per day multiplied by predicted average individual weight from the GAM:

$$_{\text{Immigration}}B_{\text{day i}} = {}_{\text{Immigration}}N_{\text{day i}} \times {}_{\text{GAM}}Wt_{\text{day i}}$$

All numbers N are themselves derived from the daily average individual weights, therefore the estimation automatically factors in that those squid immigrating on a given day would likely be smaller than average (because younger). Confidence intervals of the immigration estimates were calculated by applying the above algorithms to the MCMC iterations of the depletion models. Resulting biomasses of *D. gahi* immigration north and south, up to season end (day 252), were:

$$_{\text{Immigration}}B_{\text{N season}} = -619 \text{ t} \sim 95\% \text{ CI } [-1099 \text{ to } 7] \text{ t} \quad \textbf{(9-N)}$$

In the north, total estimated immigration was – by a narrow margin – not significantly different from zero (95% confidence interval bracketing zero), consistent with the absence of a defined in-season immigration day. However, 469 t of the negative 619 t net emigration occurred in the four-day period of August 11th to August 14th (day 223 to 226), suggesting a dispersal similar to the south following the intense bad-weather episode.

$$_{\text{Immigration}}B_{\text{S season}} = -6{,}394 \text{ t} \sim 95\% \text{ CI } [-14{,}078 \text{ to } -1{,}501] \text{ t} \quad \textbf{(9-S)}$$

In the south, the net emigration of 6,394 t in the south was almost entirely attributed to the second depletion start day (day 220; 6284 t). The estimated *D. gahi* abundance in that emigration, 0.159×10^9, was from that day on subject only to natural mortality M, and multiplied by the daily average weight[d], decreased by season end on September 9th to 5288 t. The biomass decrease is shallow (Figure 9) as the numbers declining through natural mortality were offset by the steadily increasing average weight (Figure A1-south). The immigration on day 248 was estimated at 481 t[e].

Escapement biomass

Total escapement biomass is normally defined as the aggregate biomass of *D. gahi* remaining at the end of the commercial fishing season for north and south sub-areas combined (Equations **8-N** and **8-S**). In this season, the ostensibly dispersed additional biomass presents an ambiguous quantity. Roa-Ureta (2012) discussed the possibility of emigration events, but disadvised modelling negative immigration starts because squid considered escaped could subsequently re-enter the fishing zone and be counted twice. Re-entry may not be a strongly confounding factor, as *D. gahi* migrate unidirectionally into deeper water during growth and maturation (Hatfield et al. 1990), but it also cannot be accounted whether all 'early' escapees would ultimately re-join the spawning stock. To cover the range of possible outcomes, escapement biomass for this season was assumed within the interval of two limit points: in-zone season-end biomass only, and in-zone season-end biomass plus all ostensibly dispersed biomass from the south on August 8th and still alive at season-end.

Depletion models are calculated on the inference that all fishing and natural mortality are gathered at mid-day, thus a half day of mortality ($e^{-M/2}$) was added to correspond to the closure of the fishery at 23:59 (mid-night) on September 9th.

For in-zone season-end biomass only:

$$\begin{aligned} B_{\text{Total day 252}} &= (B_{\text{S day 252}} + B_{\text{N day 252}}) \times e^{-M/2} \\ &= 9{,}568 \text{ t} \times 0.99336 \\ &= 9{,}505 \text{ t} \sim 95\% \text{ CI } [6{,}518 - 27{,}963] \text{ t} \end{aligned} \quad \textbf{(10)}$$

For in-zone season-end biomass plus dispersed biomass:

$$\begin{aligned} B_{\text{Total and Dispersed day 252}} &= (B_{\text{S day 252}} + B_{\text{N day 252}} + B_{\text{S Dispersed day 252}}) \times e^{-M/2} \\ &= 14{,}856 \text{ t} \times 0.99336 \\ &= 14{,}757 \text{ t} \sim 95\% \text{ CI } [8{,}350 - 40{,}416] \text{ t} \end{aligned} \quad \textbf{(11)}$$

North and south biomass season time series had strong positive correlation (compare Figures 7 and 9): R = +0.9550 for in-zone biomass only and R = +0.9551 for in-zone biomass

[d] Whereby it is assumed by default (albeit unverifiably) that *D. gahi* which emigrated out of the fishing zone followed the same weight progression as *D. gahi* which remained in the fishing zone.

[e] If the depletion model was run without the emigration on day 220, i.e., only with immigration starts on days 210 and 248, then the overall biomass time series was lower per day but the net immigration on day 248 was higher. All immigration starts have some influence on each other in the model, but the computational interaction between an ostensible emigration and immigrations that follow it would call for more examination.

plus dispersed biomass. Semi-randomized addition of the north and south distributions gave the aggregate likelihoods of total escapement biomass shown in Figure 10, corresponding to Equations **10** and **11**. The risk of the fishery in the current season, defined as the proportion of the total escapement biomass distribution below the conservation limit of 10,000 tonnes (Agnew et al., 2002; Barton, 2002), was calculated as 36.6% considering in-zone biomass only, and 6.6% considering in-zone biomass plus dispersed biomass.

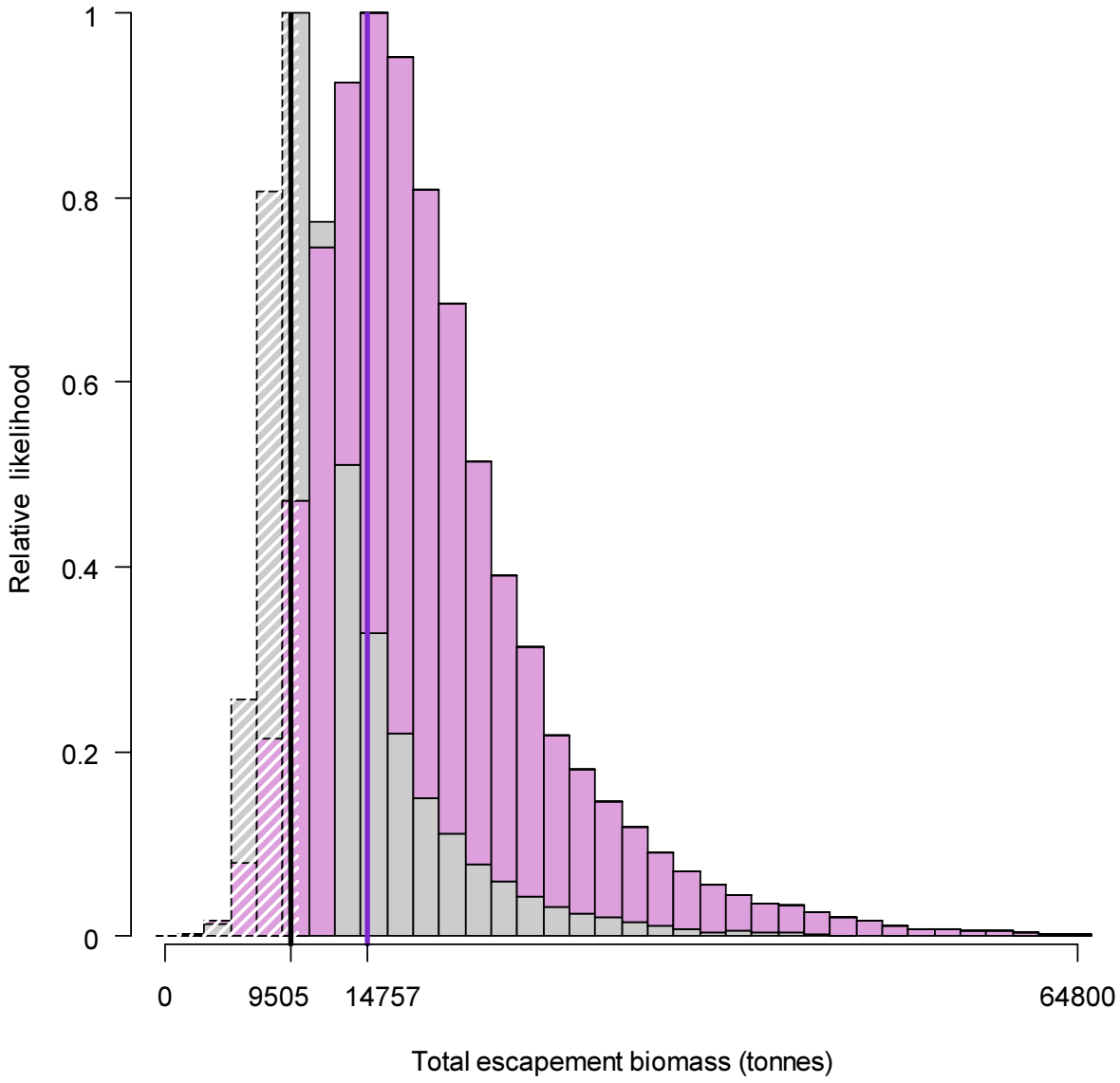

Figure 10. Likelihood distributions of total *D. gahi* escapement biomass at the season end (September 9th). Grey bars: in-zone season-end biomass only, corresponding to Equation **10**. Pale purple bars: in-zone season-end biomass plus dispersed biomass, corresponding to Equation **11**. White shading: portion of the distribution < 10,000 tonnes; equal to 36.6% of the grey distribution and 6.6% of the pale purple distribution.

The current season is the first since 2nd season in 2015 to be closed by emergency order, and the first since the onset of high pinniped numbers in the calamari fishery

(Arkhipkin et al. 2018). For this reason pinnipeds would not appear to be a cause, and other studies have found little sensitivity of fishery yields to increased presence of marine mammals (Stäbler et al. 2019). The current season also yielded the highest catch and average CPUE of any season closed by emergency order since at least 2004 (Table 1). The decision for emergency closure was taken on September 2nd, from data through September 1st (day 244). At that point the forward-projection of biomass time series indicated that the aggregate total of in-zone biomass plus dispersed biomass, i.e. the upper limit of biomass estimate, would decrease <10,000 t by September 9th. The subsequent increase of this estimate (Equation **11**) was produced by the modest immigration recorded in the south on Sept. 5th.

Pinniped bycatch

Pinniped bycatch during 2nd season 2019 totalled 7 reported fishing mortalities; 6 South American fur seals (*Arctocephalus australis*) and 1 Southern sea lion (*Otaria flavescens*), distributed as summarized in Table 2 and Figure 11. The distribution of pinniped fishing mortalities was analysed for correlation with SEDs, aggregation by trawl and by vessel, daylight[f], position proximity (latitude / longitude), trawl duration, and sea state. Correlations were tested by randomly re-distributing 100000× the pinniped mortalities among the 1881 commercial trawls during the season and calculating the proportions of the 100000 iterations that exceeded the empirical parameters[g]. The non-overlap between South American fur seal and Southern sea lion mortalities (Table 2) was also tested by these randomized re-distributions. All tests except non-overlap were calculated separately for the two pinniped species. Because the analysis implied multiple comparisons among stochastically independent null hypotheses, significance thresholds were adjusted by the Šidák correction:

$$\alpha_{corr} = 1 - (1 - \alpha)^{\frac{1}{m}} = 1 - (1 - 0.05)^{\frac{1}{5}} = 0.0102 \qquad \textbf{(12-ARA)}$$

or

$$\alpha_{corr} = 1 - (1 - \alpha)^{\frac{1}{m}} = 1 - (1 - 0.05)^{\frac{1}{2}} = 0.0253 \qquad \textbf{(12-OTB)}$$

where α = the standard significance threshold of p = 0.05, and m = number of independent null hypotheses: SED, daylight, position, duration, sea state; thus m = five[h] for South American fur seals and m = three[i] for Southern sea lions The analysis was restricted to mortalities as live captures are ambiguous to quantify: escapees cannot be counted accurately and the same animals may be caught repeatedly (especially if they're habituated, therefore non-independence of counts).

[f] Daylight is defined as a trawl hauled between sunrise and sunset, calculated using the algorithms of the NOAA Earth System research laboratory, www.esrl.noaa.gov/gmd/grad/solcalc/calcdetails.html.

[g] Either counts or weighted means.

[h] Latitude and longitude, although computed separately, were considered part of the same position parameter, therefore only one null hypothesis including both. Aggregation of trawls and vessels were tested for South American fur seal but unlike the other parameters are not potential causative agents of mortality, therefore not part of the same 'family' of null hypotheses. As vessels are nested within trawls there was also no separate 2-fold significance correction for trawl and vessel aggregation.

[i] Given a single mortality of this species (Table 2), only null hypotheses were relevant to test that a priori had an (adjusted) 5% threshold. Non-daylight was 808 out of 1881 trawls = 42.95%, non-SED was 58 out of 1881 trawls = 3.08%; thus these two hypotheses were not tested. Position proximity, and aggregation of trawls and vessels, were also not tested for Southern sea lion as a single mortality has no frame of reference against these criteria.

Table 2. Reported fishing mortalities of pinnipeds, by trawl, in 2nd season 2019.

Date	Species	No.	Grid at shoot
Jul 29th	South American fur seal	1	XVAJ
Jul 29th	South American fur seal	1	XVAL
Aug 1st	South American fur seal	1	XVAK
Aug 12th	South American fur seal	1*†	XVAL
Aug 21st	Southern sea lion	1*	XMAQ
Aug 22nd	South American fur seal	1	XTAN
Aug 26th	South American fur seal	1	XRAP

* Recaptured carcasses as evident by their state of decomposition. Accordingly it can only be assumed that the recapture grid is the same grid they were killed in.
† This animal bore marks of having being killed by a propeller. Therefore, it would not have been one of the previous captures[j].

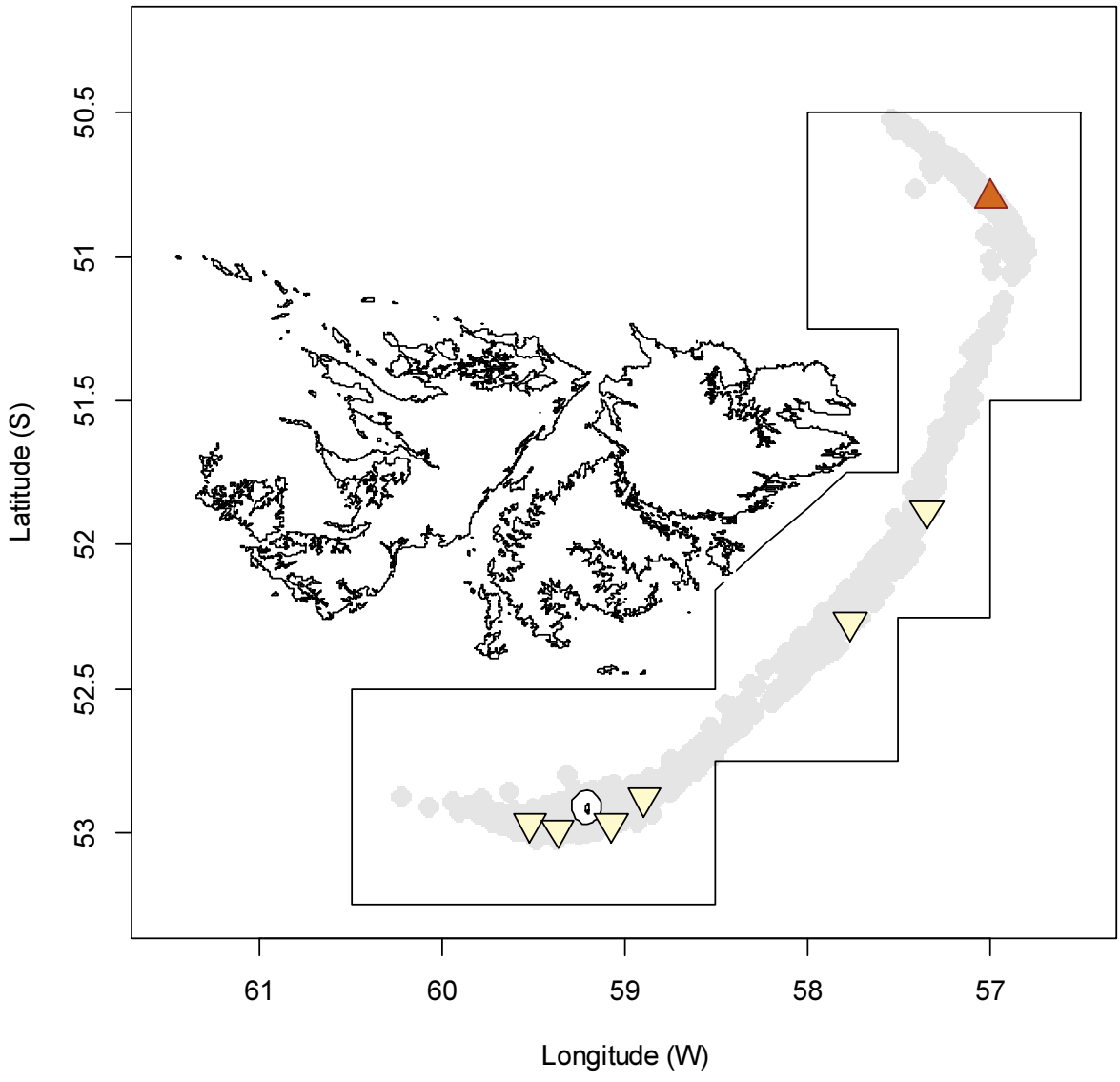

[j] In any case, vessels follow the protocol of removing a flipper from dead animals that have been recovered on deck before discharging them, to prevent prior mortalities from being re-counted.

Figure 11 [previous page]. Distribution of pinniped trawl mortalities during 2nd season 2019. South American fur seals: off-white, point-down. Southern sea lion: brown, point-up. Grey under-shading: distribution of trawls, equivalent to Figure 2.

Pinniped mortalities were not aggregated by trawl as every South American fur seal and Southern sea lion was reported killed in a different trawl. Pinniped mortalities were also not significantly aggregated by vessel as the six South American fur seals were taken on four different vessels (one vessel out of 17 took 3 and three other vessels took 1 each), and the Southern sea lion was taken on a further different vessel. None of the correlative null hypotheses were statistically significant at the given p-value thresholds (Table 3). It could be argued that the SED factor for South American fur seals, at $p = 0.013$, would be significant if the other null hypotheses had not been bothered with in the first place. The inclusion of parallel null hypotheses is a matter of some subjectivity (Frane 2015), and daylight, trawl duration, and sea state had not shown significance in previous seasons (Winter 2018b, 2019). However, the caveat still applies that significance of SED improvement is potentially biased because SED implementation was triggered by the precedence of mortalities, rather than assigned a priori, and therefore confounded with chronological progression as SEDs remained continually in use once they started to be used. In comparison to the three previous seasons (Winter 2018a, 2018b, 2019), South American fur seals in this season were caught further north in the central part of the Loligo Box, whereas the Southern sea lion was again typically caught in the north (Figure 11). The absence of overlap between South American fur seal and Southern sea lion mortalities in this season corresponded to >95% of randomizations (Table 3), suggesting that relative distributions of the two species are oppositional.

Table 3. Hypotheses correlating pinniped mortalities in the 2nd season 2019 commercial fishery. Outcomes are either the mortality counts or the mortality-weighted means of that hypothesis parameter. Non-significant parameters are shaded grey.

Mortality hypothesis	South American fur seal		Southern sea lion	
	Outcome	p	Outcome	p
Without SED	2 / 6	0.0130	-	-
Trawl aggregation[a]	6 / 1881	1.0000	-	-
Vessel aggregation[b]	4 / 17	>0.1500	-	-
Daylight	3 / 6	>0.5000	-	-
Lat / Lon position	52.66ºS × 58.66ºW	>0.2500	50.80ºS × 56.99ºW	-
Trawl duration	3.75 hours	>0.0300	5.50 hours	>0.5000
Sea state[c]	3.17	>0.2500	2.00	>0.0600
Both species				
Non-overlap	0 / 7	>0.9500	-	-

[a] See Table 2.
[b] Vessels not identified, for confidentiality.
[c] Beaufort wind force scale.

Seabird bycatch

Seabird bycatch during 2nd season 2019 totalled 4 reported fishing mortalities; 3 black-browed albatross (*Thalassarche melanophrys*) and 1 Gentoo penguin (*Pygoscelis papua*),

distributed as summarized in Table 4. The four mortalities were reported on three different vessels.

Table 4. Reported fishing mortalities of seabirds, by trawl, in 2nd season 2019.

Date	Species	No.	Grid at shoot
Aug 13th	Black-browed albatross	1	XLAP
Aug 22nd	Black-browed albatross	1*	XTAN
Aug 31st	Black-browed albatross	1†	XRAP
Sep 2nd	Gentoo penguin	1†	XWAK

* Entangled and killed during hauling.
† Killed in shoot, did not escape through SED hatch.

Fishery bycatch

All 635 2nd season vessel-days (Table 1) reported *D. gahi* squid as their primary catch. The proportion of total catch represented by *D. gahi* (24748100/25004798 = 0.990; Table A1) is slightly lower than 1st season but higher than in both seasons in 2018. Highest bycatches in 2nd season 2019 were common hake *Merluccius hubbsi* with 90 t reported from 472 vessel-days, rock cod *Patagonotothen ramsayi* (78 t, 565 vessel-days), red cod *Salilota australis* (35 t, 135 vessel-days), skate Rajiformes (18 t, 440 vessel-days), medusae (8 t, 130 vessel-days), hoki *Macruronus magellanicus* (7 t, 48 vessel-days), kingclip *Genypterus blacodes* (7 t, 105 vessel-days), and frogmouth *Cottoperca gobio* (3 t, 280 vessel-days). Relative distributions by grid of these bycatches are shown in Figure 12, and the complete list of all catches by species is given in Table A1.

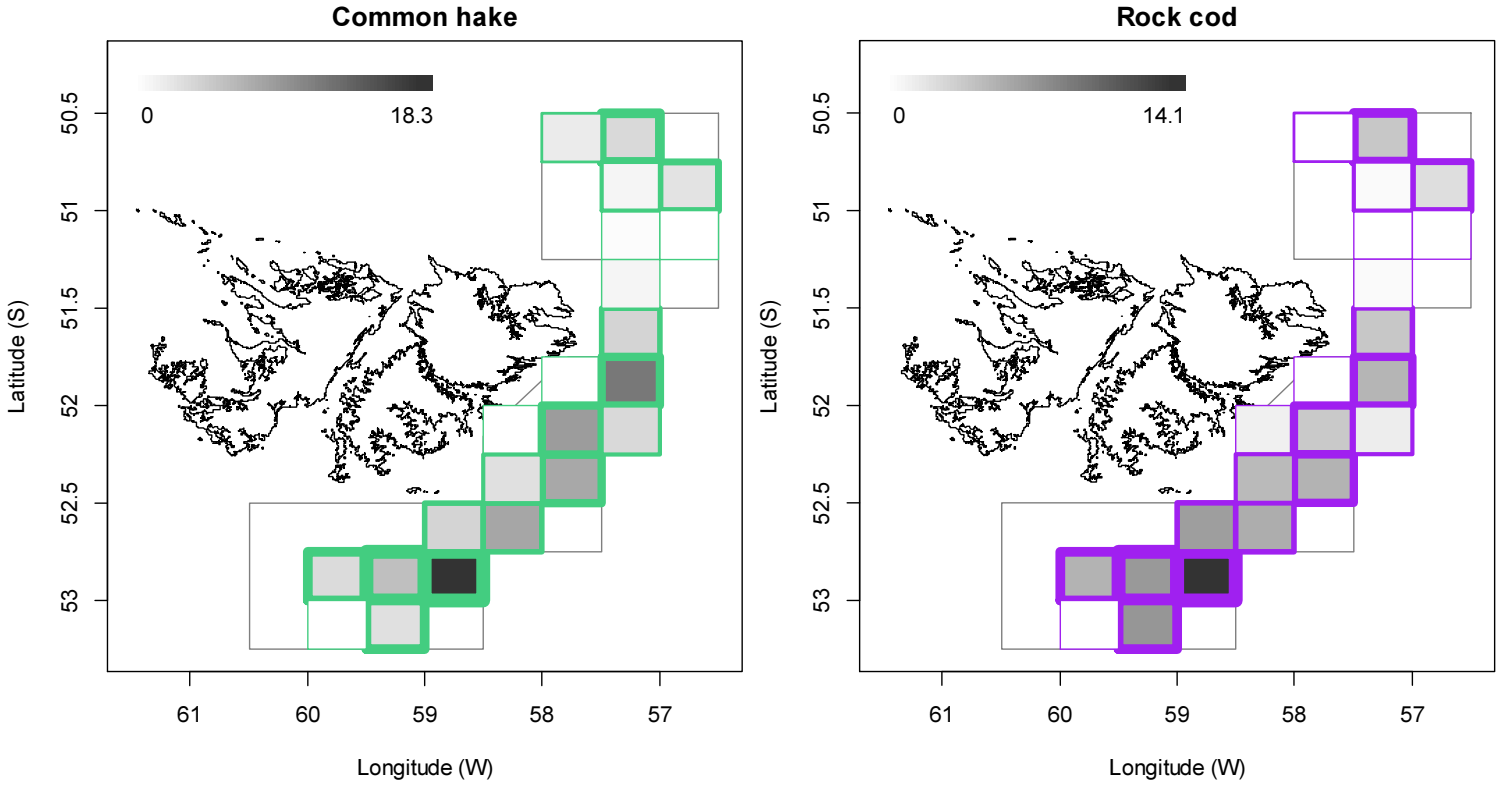

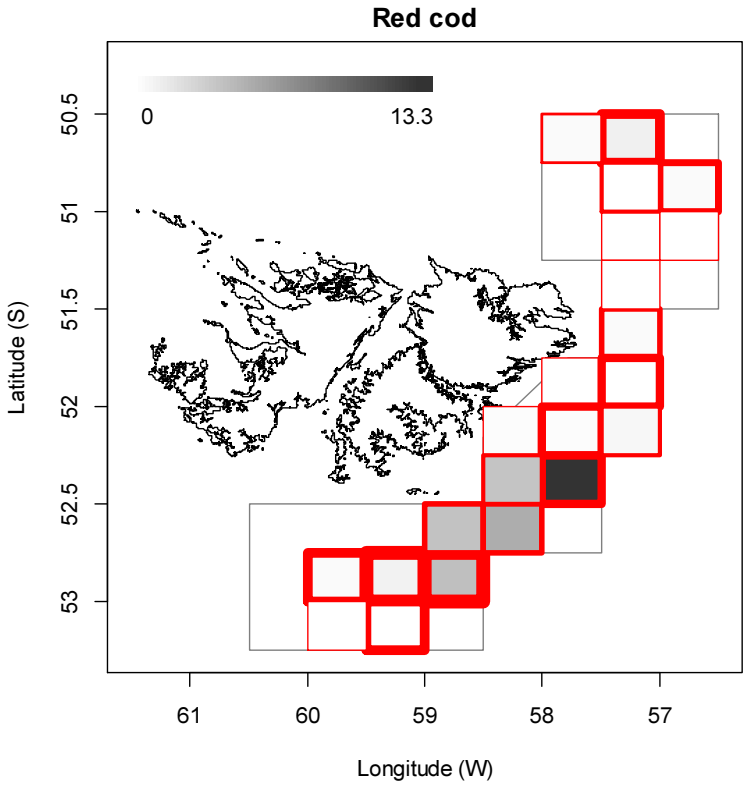
Red cod
0
13.3
Latitude (S)
50.5
51
51.5
52
52.5
53
61
60
59
58
57
Longitude (W)

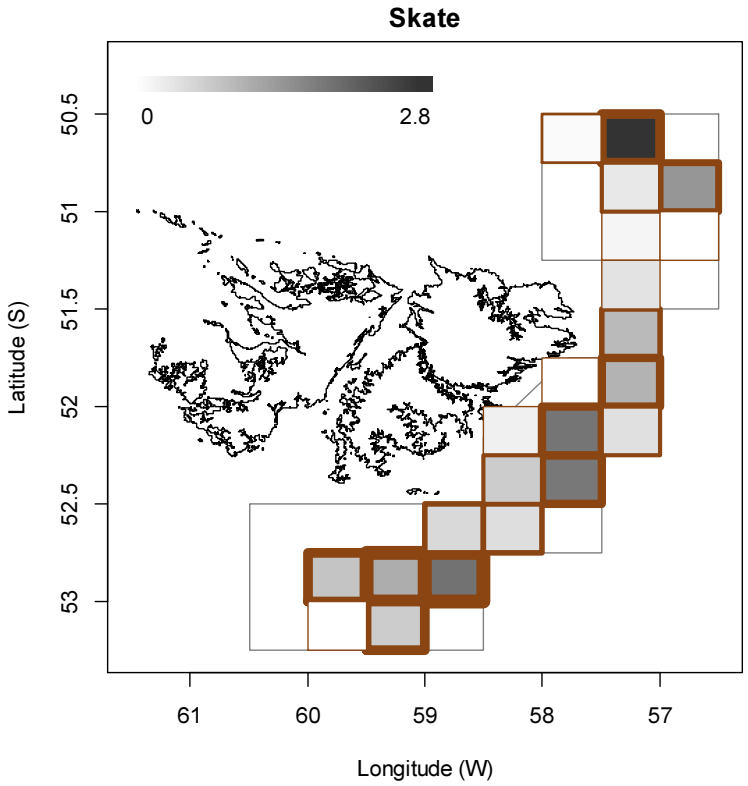
Skate
0
2.8
Latitude (S)
50.5
51
51.5
52
52.5
53
61
60
59
58
57
Longitude (W)

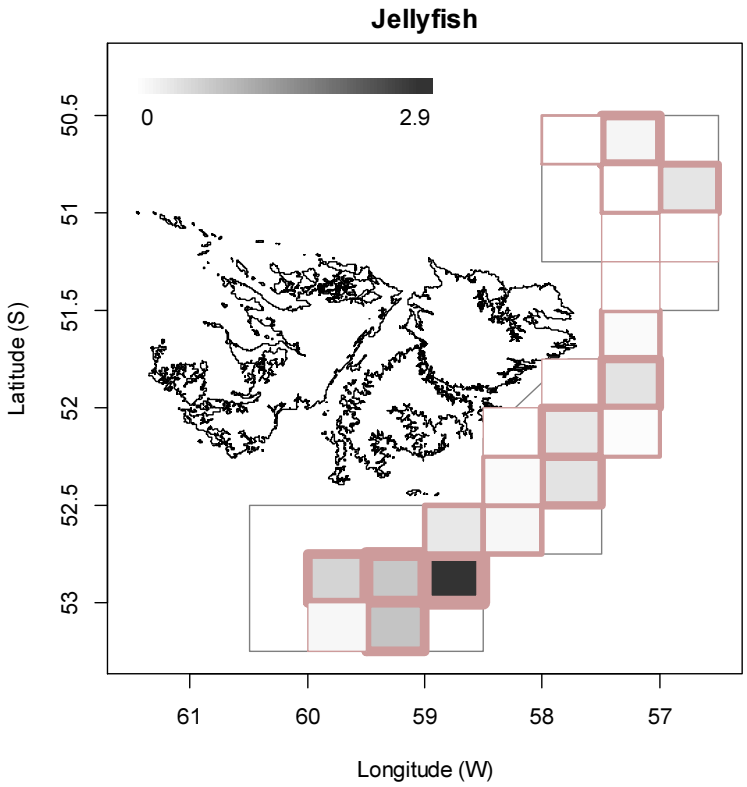
Jellyfish
0
2.9
Latitude (S)
50.5
51
51.5
52
52.5
53
61
60
59
58
57
Longitude (W)

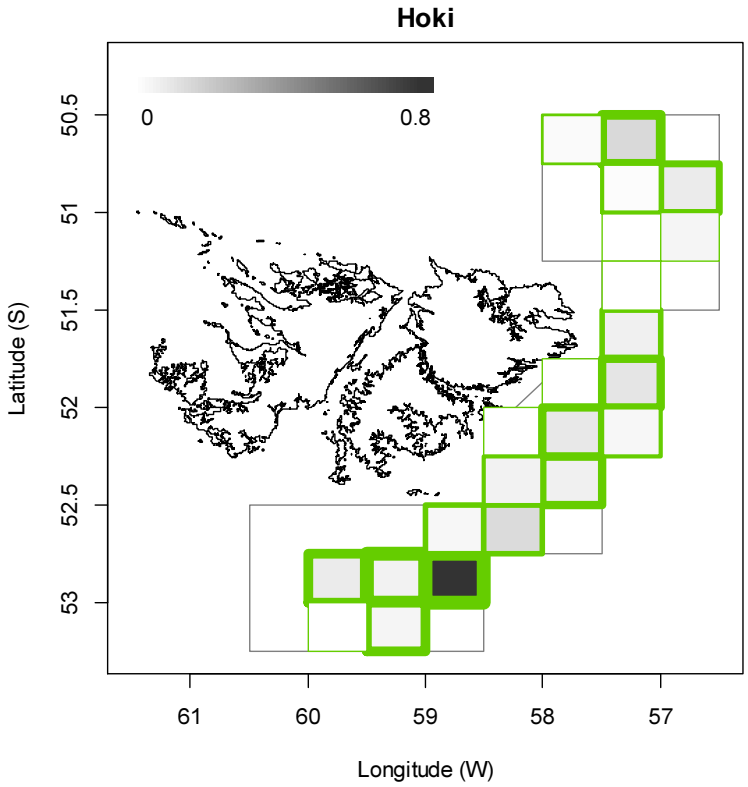
Hoki
0
0.8
Latitude (S)
50.5
51
51.5
52
52.5
53
61
60
59
58
57
Longitude (W)

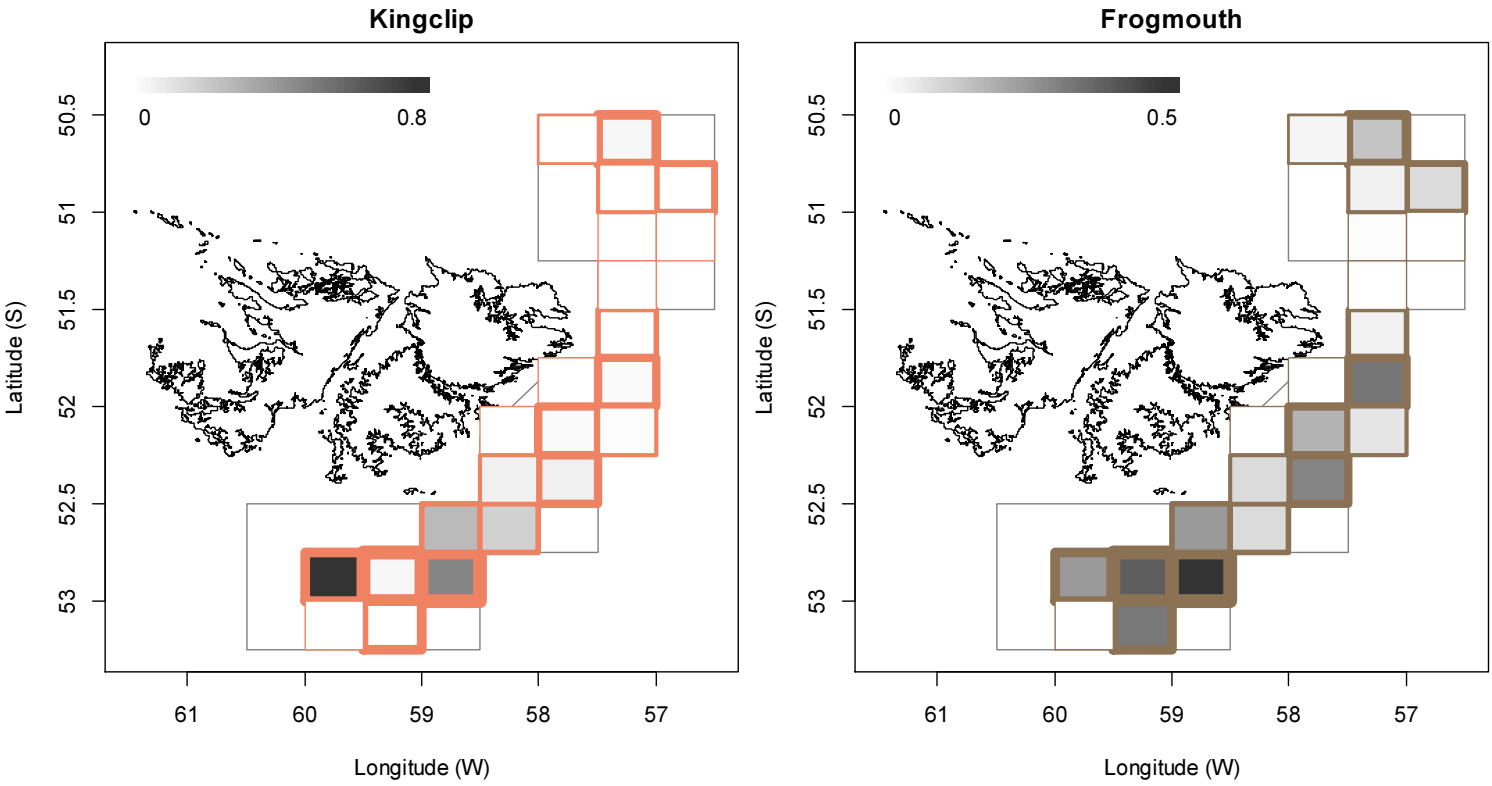

Figure 12. Distributions of the eight principal bycatches during 2nd season 2019, by noon position grids. Thickness of grid lines is proportional to the number of vessel-days (1 to 108 per grid; 22 different grids were occupied). Grey-scale is proportional to the bycatch biomass; maximum (tonnes) indicated on each plot.

Trawl area coverage

The impact of bottom trawling on seafloor habitat has been a matter of concern in commercial fisheries (Kaiser et al. 2002; 2006), whereby the potential severity of impact relates to spatial and temporal extents of trawling (Piet and Hintzen 2012, Gerritsen et al. 2013). For the *D. gahi* fishery, available catch, effort, and positional data are used to summarize the estimated 'ground' area coverage occupied during the season of trawling.

The procedure for summarizing trawl area coverage is described in the Appendix. 50% of total *D. gahi* catch was taken from 1.3% of the total area of the Loligo Box, corresponding approximately[k] to the aggregate of grounds trawled ≥7.8 times. 90% of total *D. gahi* catch was taken from 6.9% of the total area of the Loligo Box, corresponding approximately to the aggregate of grounds trawled ≥2.5 times. 100% of total *D. gahi* catch over the season was taken from 11.7% of the total area of the Loligo Box, obviously corresponding to the aggregate of all grounds trawled at least once (Figure 13 - left). Averaged by 5 × 5 km grid (Figure 13 - right), 4 grids (out of 1383) had coverage of 10 or more (that is to say, every patch of ground within that 5 × 5 km was on average trawled over ≥10 times or more). Twenty-six grids had coverage of 5 or more, and 82 grids had coverage of 2 or more.

[k] However, not exactly. There is an expected strong correlation between the density of *D. gahi* catch taken from area units and how often these area units were trawled, but the correlation is not perfectly monotonic.

The concentration of all *D. gahi* catch into 11.7% of area, while still high, is noticeably lower than in the previous two seasons undertaken with this type of analysis: 1st season 2018 (7.1%), and 1st season 2019 (7.7%). Both of those seasons reported very high catches and high escapement biomass (Winter 2018a, Winter 2019). The outcome suggests a direct correlation with fishing success: in a season ending with low catches vessels cover more ground searching.

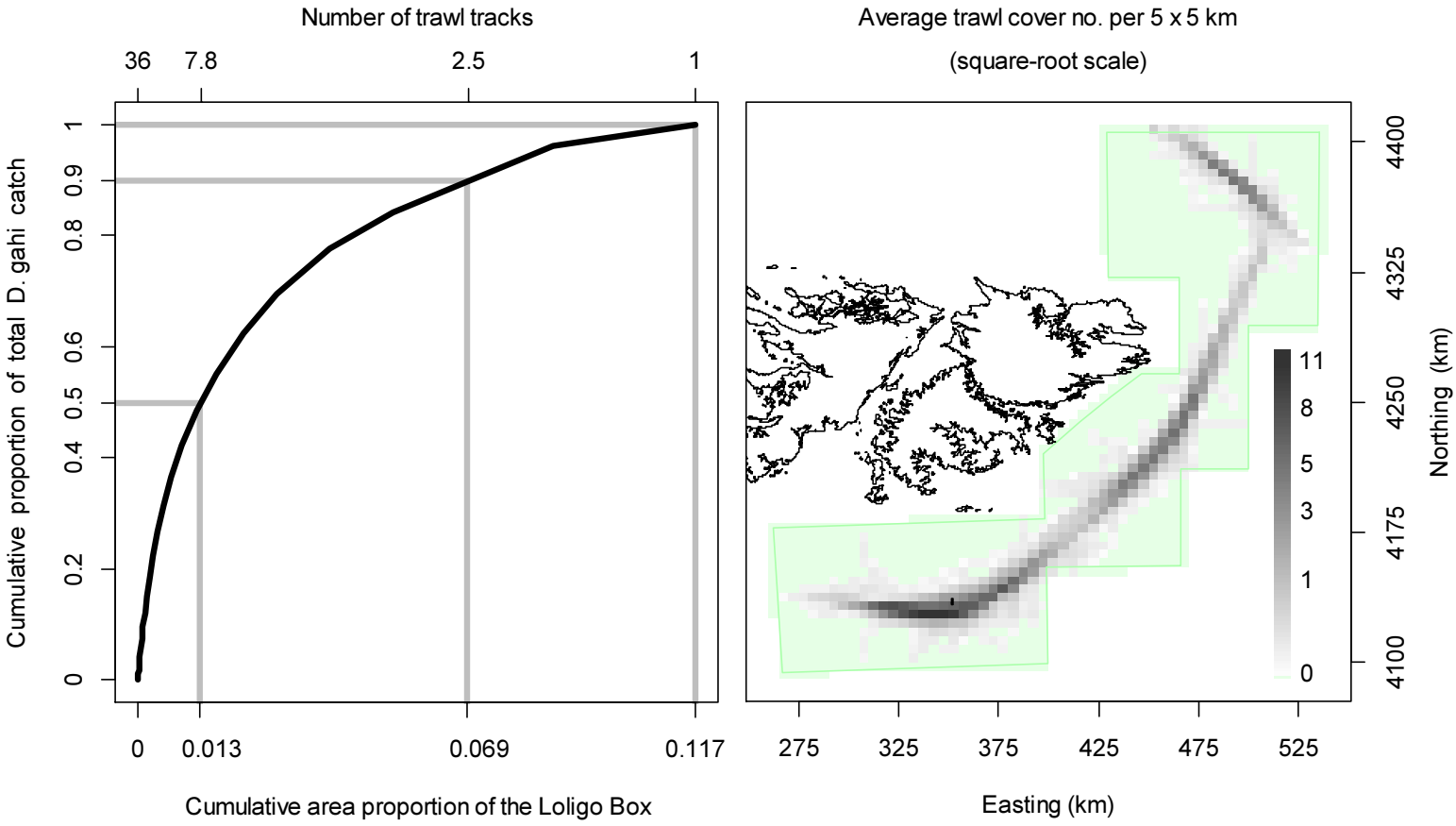

Figure 13. Left: cumulative *D. gahi* catch of 2nd season 2019, vs. cumulative area proportion of the Loligo Box the catch was taken from. The maximum number of times that any single area unit was trawled was 36, and catch cumulation by reverse density corresponded approximately to the trawl multiples shown on the top x-axis. Right: trawl cover averaged by 5 × 5 km grid; green area represents zero trawling.

References

Agnew, D.J., Baranowski, R., Beddington, J.R., des Clers, S., Nolan, C.P. 1998. Approaches to assessing stocks of *Loligo gahi* around the Falkland Islands. Fisheries Research 35: 155-169.

Agnew, D. J., Beddington, J. R., and Hill, S. 2002. The potential use of environmental information to manage squid stocks. Canadian Journal of Fisheries and Aquatic Sciences, 59: 1851–1857.

Arkhipkin, A. 1993. Statolith microstructure and maximum age of *Loligo gahi* (Myopsida: Loliginidae) on the Patagonian Shelf. Journal of the Marine Biological Association of the UK 73: 979-982.

Arkhipkin, A.I., Blake, D., Iriarte, V. 2018. Introduction of seal exclusion devices to avoid seal bycatch in squid trawling fishery in the Falkland Islands. ICES CM 2018/N: 33.

Arkhipkin, A.I., Middleton, D.A.J. 2002. Sexual segregation in ontogenetic migrations by the squid *Loligo gahi* around the Falkland Islands. Bulletin of Marine Science 71: 109-127.

Arkhipkin, A.I., Middleton, D.A.J., Barton, J. 2008. Management and conservation of a short-lived fishery resource: *Loligo gahi* around the Falkland Islands. American Fisheries Society Symposium 49: 1243-1252.

Barton, J. 2002. Fisheries and fisheries management in Falkland Islands Conservation Zones. Aquatic Conservation: Marine and Freshwater Ecosystems 12: 127–135.

Brooks, S.P., Gelman, A. 1998. General methods for monitoring convergence of iterative simulations. Journal of computational and graphical statistics 7:434-455.

Chen, X., Chen, Y., Tian, S., Liu, B., Qian, W. 2008. An assessment of the west winter-spring cohort of neon flying squid (*Ommastrephes bartramii*) in the Northwest Pacific Ocean. Fisheries Research 92: 221-230.

DeLury, D.B. 1947. On the estimation of biological populations. Biometrics 3: 145-167.

Frane, A.V. 2015. Planned hypothesis tests are not necessarily exempt from multiplicity adjustment. Journal of Research Practice 11: P2.

Gamerman, D., Lopes, H.F. 2006. Markov Chain Monte Carlo. Stochastic simulation for Bayesian inference. 2nd edition. Chapman & Hall/CRC.

Gerritsen, H.D., Minto, C., Lordan, C. 2013. How much of the seabed is impacted by mobile fishing gear? Absolute estimates from Vessel Monitoring System (VMS) point data. ICES Journal of Marine Science 70: 523-531.

Goyot, L., Derbyshire, C., Jones, J., Tutjavi, V., Winter, A. 2019. *Doryteuthis gahi* stock assessment survey, 2nd season 2019. Technical Document, Falkland Islands Fisheries Dept. 20 p.

Hatfield, E.M.C., Rodhouse, P.G., Porebski, J. 1990. Demography and distribution of the Patagonian squid (*Loligo gahi* d'Orbigny) during the austral winter. Journal du Conseil international pour l'Exploration de la Mer 46 : 306-312.

Hoenig, J.M. 1983. Empirical use of longevity data to estimate mortality rates. Fishery Bulletin 82: 898-903.

Kairua, T. 2019. Observer Report 1239. Technical Document, FIG Fisheries Department. 21 p.

Kaiser, M.J., Collie, J.S., Hall, S.J., Jennings, S., Poiner, I.R. 2002. Modification of marine habitats by trawling activities: prognosis and solutions. Fish and Fisheries 3: 114-136.

Kaiser, M.J., Clarke, K.R., Hinz, H., Austen, M.C.V., Somerfield, P.J., Karakassis, I. 2006. Global analysis of response and recovery of benthic biota to fishing. Marine Ecology Progress Series 311: 1-14.

Keller, S., Robin, J.P., Valls, M., Gras, M., Cabanellas-Reboredo, M., Quetglas, A. 2015. The use of depletion models to assess Mediterranean cephalopod stocks under the current EU data collection framework. Mediterranean Marine Science 16: 513-523.

Magnusson, A., Punt, A., Hilborn, R. 2013. Measuring uncertainty in fisheries stock assessment: the delta method, bootstrap, and MCMC. Fish and Fisheries 14: 325-342.

Medellín-Ortiz, A., Cadena-Cárdenas, L., Santana-Morales, O. 2016. Environmental effects on the jumbo squid fishery along Baja California's west coast. Fisheries Science 82: 851-861.

Morales-Bojórquez, E., Hernández-Herrera, A., Cisneros-Mata, M.A., Nevárez-Martínez, M.O. 2008. Improving estimates of recruitment and catchability of jumbo squid *Dosidicus gigas* in the Gulf of California, Mexico. Journal of Shellfish Research 27: 1233-1237.

Nash, J.C., Varadhan, R. 2011. optimx: A replacement and extension of the optim() function. R package version 2011-2.27. http://CRAN.R-project.org/package=optimx

Patterson, K.R. 1988. Life history of Patagonian squid *Loligo gahi* and growth parameter estimates using least-squares fits to linear and von Bertalanffy models. Marine Ecology Progress Series 47: 65-74.

Payá, I. 2010. Fishery Report. *Loligo gahi*, Second Season 2009. Fishery statistics, biological trends, stock assessment and risk analysis. Technical Document, Falkland Islands Fisheries Dept. 54 p.

Pebesma, E., bivand, R., Rowlingson, B., Gomez-Rubio, V., Hijmans, R., Sumner, M., MacQueen, D., Lemon, J., O'Brien, J., O'Rourke, J. 2018. Classes and Methods for Spatial Data. R package version 1.3-1. https://cran.r-project.org/web/packages/sp/index.html.

Pierce, G.J., Guerra, A. 1994. Stock assessment methods used for cephalopod fisheries. Fisheries Research 21: 255 – 285.

Piet, G.J., Hintzen, N.T. 2012. Indicators of fishing pressure and seafloor integrity. ICES Journal of Marine Science 69: 1850-1858.

Punt, A.E., Hilborn, R. 1997. Fisheries stock assessment and decision analysis: the Bayesian approach. Reviews in Fish Biology and Fisheries 7:35-63.

Roa-Ureta, R. 2012. Modelling in-season pulses of recruitment and hyperstability-hyperdepletion in the *Loligo gahi* fishery around the Falkland Islands with generalized depletion models. ICES Journal of Marine Science 69: 1403–1415.

Roa-Ureta, R., Arkhipkin, A.I. 2007. Short-term stock assessment of *Loligo gahi* at the Falkland Islands: sequential use of stochastic biomass projection and stock depletion models. ICES Journal of Marine Science 64: 3-17.

Rosenberg, A.A., Kirkwood, G.P., Crombie, J.A., Beddington, J.R. 1990. The assessment of stocks of annual squid species. Fisheries Research 8: 335-350.

Royer, J., Périès, P., Robin, J.P. 2002. Stock assessments of English Channel loliginid squids: updated depletion methods and new analytical methods. ICES Journal of Marine Science 59: 445-457.

Shaw, P.W., Arkhipkin, A.I., Adcock, G.J., Burnett, W.J., Carvalho, G.R., Scherbich, J.N., Villegas, P.A. 2004. DNA markers indicate that distinct spawning cohorts and aggregations of Patagonian squid, *Loligo gahi*, do not represent genetically discrete subpopulations. Marine Biology, 144: 961-970.

Stäbler, M., Kempf, A., Smout, S., Temming, A. 2019. Sensitivity of multispecies maximum sustainable yields to trends in the top (marine mammals) and bottom (primary production) compartments of the southern North Sea foodweb. PLoS ONE 14(1): e0210882.

Swartzman, G., Huang, C., Kaluzny, S. 1992. Spatial analysis of Bering Sea groundfish survey data using generalized additive models. Canadian Journal of Fisheries and Aquatic Sciences 49: 1366-1378.

Tutjavi, V. 2019. Observer Report 1238. Technical Document, FIG Fisheries Department. 24 p.

Winter, A. 2014. *Loligo* stock assessment, second season 2014. Technical Document, Falkland Islands Fisheries Department. 30 p.

Winter, A. 2017a. Stock assessment – Falkland calamari (*Doryteuthis gahi*). Technical Document, Falkland Islands Fisheries Department. 30 p.

Winter, A. 2018a. Stock assessment – *Doryteuthis gahi* 1st season 2018. Technical Document, Falkland Islands Fisheries Department. 36 p.

Winter, A. 2018b. Stock assessment – *Doryteuthis gahi* 2nd season 2018. Technical Document, Falkland Islands Fisheries Department. 34 p.

Winter, A. 2019. Stock assessment – *Doryteuthis gahi* 1st season 2019. Technical Document, Falkland Islands Fisheries Department. 37 p.

Winter, A., Arkhipkin, A. 2015. Environmental impacts on recruitment migrations of Patagonian longfin squid (*Doryteuthis gahi*) in the Falkland Islands with reference to stock assessment. Fisheries Research 172: 85-95.

Young, I.A.G., Pierce, G.J., Daly, H.I., Santos, M.B., Key, L.N., Bailey, N., Robin, J.-P., Bishop, A.J., Stowasser, G., Nyegaard, M., Cho, S.K., Rasero, M., Pereira, J.M.F. 2004. Application of depletion methods to estimate stock size in the squid *Loligo forbesi* in Scottish waters (UK). Fisheries Research 69: 211-227.

Appendix
***Doryteuthis gahi* individual weights**

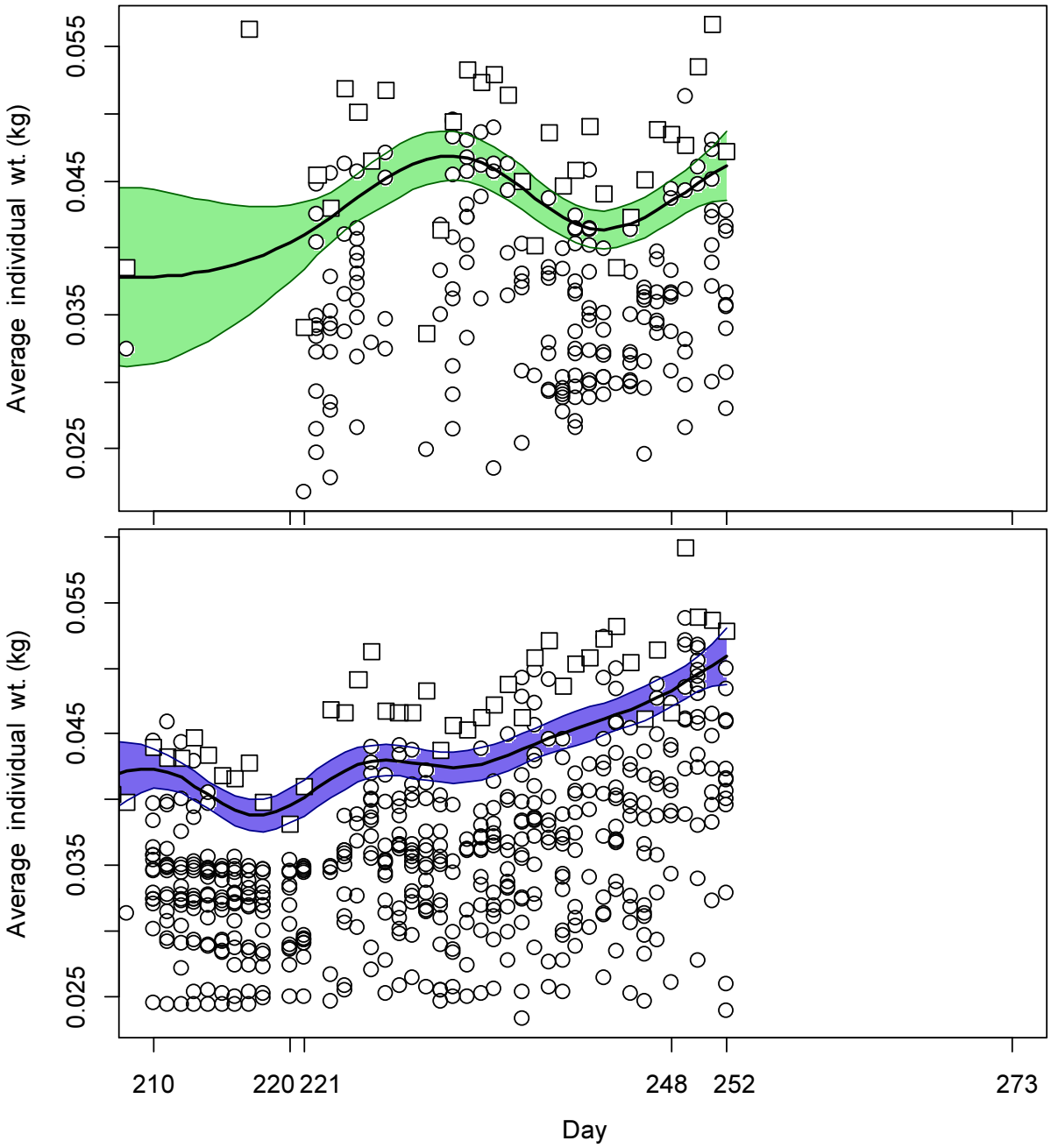

Figure A1. North (top) and south (bottom) sub-area daily average individual *D. gahi* weights from commercial size categories per vessel (circles) and observer measurements (squares). GAMs of the daily trends ± 95% confidence intervals (centre lines and colour under-shading).

To smooth fluctuations, GAM trends were calculated of daily average individual weights. North and south sub-areas were calculated separately. For continuity, GAMs were calculated using all pre-season survey and in-season data contiguously. North and south GAMs were first calculated separately on the commercial and observer data. Commercial data GAMs were taken as the baseline trends, and calibrated to observer data GAMs in proportion to the

correlation between commercial data and observer data GAMs. For example, if the season average individual weight estimate from commercial data was 0.052 kg, the season average individual weight estimate from observer data was 0.060 kg, and the coefficient of determination (R^2) between commercial and observer GAM trends was 86%, then the resulting trend of daily average individual weights was calculated as the commercial data GAM values + (0.060 – 0.052) × 0.86. This way, both the greater day-to-day consistency of the commercial data trends, and the greater point value accuracy of the observer data are represented in the calculations. GAM plots of the north and south sub-areas are shown in Figure A1.

Prior estimates and CV

The pre-season survey had estimated *D. gahi* biomasses of 18,516 t north of 52º S and 32,364 t south of 52º S (Goyot et al. 2019). Hierarchical bootstrapping of the inverse distance weighting algorithm obtained a coefficient of variation (CV) of 14.4% of the survey biomass distributions. From modelled survey catchability, Payá (2010) had estimated average net escapement of up to 22%, which was added to the CV:

$$18{,}516 \pm (.144 + .22) = 18{,}516 \pm 36.4\% = 18{,}516 \pm 6{,}744 \text{ t} \quad \textbf{(A1-N)}$$

$$32{,}364 \pm (.144 + .22) = 32{,}364 \pm 36.4\% = 32{,}364 \pm 11{,}788 \text{ t} \quad \textbf{(A1-S)}$$

The 22% escapement was added as a linear increase in the variability, but was not used to reduce the total estimate, because squid that escape one trawl are likely to be part of the biomass concentration that is available to the next trawl.

D. gahi numbers at the end of the survey were estimated as the survey biomasses divided by the GAM-predicted individual weight averages for the survey: 0.0387 kg north, 0.0413 kg south (Figure A1), and 0.0410 kg combined. Average coefficients of variation (CV) of the GAM over the duration of the pre-season survey were 7.6% north and 4.2% south. CV of the length-weight conversion relationship (Equation **7**) were 8.0% north and 8.2% south. Joining these sources of variation with the pre-season survey biomass estimates and individual weight averages (above) gave estimated *D. gahi* numbers at survey end (day 208) of:

$$_{\text{prior}}\text{N}_{\text{N day 208}} = \frac{18{,}516 \times 1000}{0.0387} \pm \sqrt{36.4\%^2 + 7.6\%^2 + 8.0\%^2}$$

$$= 0.478 \times 10^9 \pm 38.1\%$$

$$_{\text{prior}}\text{N}_{\text{S day 208}} = \frac{32{,}364 \times 1000}{0.0413} \pm \sqrt{36.4\%^2 + 4.2\%^2 + 8.2\%^2}$$

$$= 0.785 \times 10^9 \pm 37.6\%$$

Priors were normalized for the combined fishing zone average, to produce better continuity as vessels cross back and forth between north and south:

$$_{\text{nprior}}\text{N}_{\text{N day 208}} = \left(\frac{(18{,}516 + 32{,}364) \times 1000}{0.0410}\right) \times \left(\frac{_{\text{prior}}\text{N}_{\text{N day 208}}}{_{\text{prior}}\text{N}_{\text{N day 208}} + _{\text{prior}}\text{N}_{\text{S day 208}}}\right)$$

$$= 0.470 \times 10^9 \pm 38.1\% \quad \textbf{(A2-N)}$$

$${}_{\text{nprior}}N_{\text{S day 208}} = \left(\frac{(18{,}516 + 32{,}364) \times 1000}{0.0410}\right) \times \left(\frac{{}_{\text{prior}}N_{\text{S day 208}}}{{}_{\text{prior}}N_{\text{N day 208}} + {}_{\text{prior}}N_{\text{S day 208}}}\right)$$

$$= 0.772 \times 10^9 \pm 37.6\% \quad \textbf{(A2-S)}$$

The depletion time series in the north was started from day 221 (Figure 3), but as only one vessel fished north that day the catchability coefficient (q) prior was calculated from the next day (day 222) when 11 vessels fished north, giving a more stable estimate. Abundance on day 222 was discounted for natural mortality over the 14 days since the end of the survey:

$${}_{\text{nprior}}N_{\text{N day 222}} = {}_{\text{nprior}}N_{\text{N day 208}} \times e^{-M \cdot (222-208)} - \text{CNMD}_{\text{N day 208}} = 0.390 \times 10^9 \quad \textbf{(A3-N)}$$

where $\text{CNMD}_{\text{N day 222}} = 0.00047 \times 10^9$ from one day of fishing on day 221. Thus:

$${}_{\text{prior}}q_{\text{N}} = C(N)_{\text{N day 222}} / ({}_{\text{nprior}}N_{\text{N day 222}} \times E_{\text{S day 222}})$$

$$= (C(B)_{\text{N day 222}} / \text{Wt}_{\text{N day 222}}) / ({}_{\text{nprior}}N_{\text{N day 222}} \times E_{\text{N day 222}})$$

$$= (412.2 \text{ t} / 0.0416 \text{ kg}) / (0.390 \times 10^9 \times 11 \text{ vessel-days})$$

$$= 2.311 \times 10^{-3} \text{ vessels}^{-1} \quad \textbf{(A4-N)}$$ [1]

CV of the prior was calculated as the sum of variability in ${}_{\text{nprior}}N_{\text{N day 208}}$ (Equation **A2-N**) plus variability in the catches of vessels on start day + 1 = 222, plus variability of the natural mortality (see Appendix section Natural mortality, below):

$$CV_{\text{prior N}} =$$

$$\sqrt{38.1\%^2 + \left(\frac{\text{SD}\left(C(B)_{\text{N vessels day 222}}\right)}{\text{mean}\left(C(B)_{\text{N vessels day 222}}\right)}\right)^2 + (1 - \text{sign}(1 - CV_M) \times \text{abs}(1 - CV_M)^{(222-208)})^2}$$

$$= \sqrt{38.1\%^2 + 31.2\%^2 + 90.5\%^2} = 103.0\% \quad \textbf{(A5-N)}$$

The catchability coefficient (q) prior for the south sub-area was taken on day 210, the first day of the season, when 15 vessels fished in the south and the initial depletion period south started. Abundance on day 210 was discounted for natural mortality over the 2 days since the end of the survey:

$${}_{\text{nprior}}N_{\text{S day 210}} = {}_{\text{nprior}}N_{\text{S day 208}} \times e^{-M \cdot (210-208)} - \text{CNMD}_{\text{S day 210}} = 0.752 \times 10^9 \quad \textbf{(A3-S)}$$

where $\text{CNMD}_{\text{S day 210}} = 0$ as no catches intervened between the end of the survey and the start of commercial season. Thus:

$${}_{\text{prior}}q_{\text{S}} = C(N)_{\text{S day 210}} / ({}_{\text{nprior}}N_{\text{S day 210}} \times E_{\text{S day 210}})$$

[1] On Figure 6-left.

$$= (C(B)_{S\ day\ 210} / Wt_{S\ day\ 210}) / ({}_{nprior}N_{S\ day\ 210} \times E_{S\ day\ 210})$$

$$= (1314.8\ t / 0.0424\ kg) / (0.752 \times 10^{9} \times 15\ vessel\text{-}days)$$

$$= 2.753 \times 10^{-3}\ vessels^{-1}\ ^{m} \qquad \textbf{(A4-S)}$$

CV of the prior was calculated as the sum of variability in ${}_{nprior}N_{S\ day\ 208}$ (Equation **A2-S**) plus variability in the catches of vessels on start day 210, plus variability of the natural mortality (see Appendix section Natural mortality, below):

$$CV_{prior\ S} =$$

$$\sqrt{37.6\%^2 + \left(\frac{SD\left(C(B)_{S\ vessels\ day\ 210}\right)}{mean\left(C(B)_{S\ vessels\ day\ 210}\right)}\right)^2 + (1 - sign(1 - CV_M) \times abs(1 - CV_M)^{(210-208)})^2}$$

$$= \sqrt{37.6\%^2 + 23.6\%^2 + 28.5\%^2} \quad = 52.8\% \qquad \textbf{(A5-S)}$$

Depletion model estimates and CV

For the north sub-area, the equivalent of Equation **2** with one N_{day} was optimized on the difference between predicted catches and actual catches (Equation **3**), resulting in parameters values:

$${}_{depletion}N1_{N\ day\ 221} = 0.198 \times 10^{9}$$

$${}_{depletion}q_{N} = 3.323 \times 10^{-3}\ ^{n} \qquad \textbf{(A6-N)}$$

The root-mean-square deviation of predicted vs. actual catches was calculated as the CV of the model:

$$CV_{rmsd\ N} = \frac{\sqrt{\sum_{i=1}^{n}\left({}_{predicted}C(N)_{N\ day\ i} - {}_{actual}C(N)_{N\ day\ i}\right)^2 / n}}{mean\left({}_{actual}C(N)_{N\ day\ i}\right)}$$

$$= 1.021 \times 10^{6} / 2.487 \times 10^{6} = 41.1\% \qquad \textbf{(A7-N)}$$

$CV_{rmsd\ N}$ was added to the variability of the GAM-predicted individual weight averages for the season (Figure A1-N); equal to a CV of 2.1% north. CVs of the depletion were then calculated as the sum:

$$CV_{depletion\ N} = \sqrt{CV_{rmsd\ N}^{\ 2} + CV_{GAM\ Wt\ N}^{\ 2}} = \sqrt{41.1\%^2 + 2.1\%^2}$$

$$= 41.1\% \qquad \textbf{(A8-N)}$$

[m] On Figure 8-left.
[n] On Figure 6-left.

For the south sub-area, the equivalent of Equation **2** with three N_{day} was optimized on the difference between predicted catches and actual catches (Equation **3**), resulting in parameters values:

$$_{depletion}N1_{S\ day\ 210} = 0.695 \times 10^9; \quad _{depletion}N2_{S\ day\ 220} = -0.014 \times 10^9$$
$$_{depletion}N3_{S\ day\ 248} = 0.022 \times 10^9$$
$$_{depletion}q_S = 4.315 \times 10^{-3}\ ^{o} \qquad \textbf{(A6-S)}$$

The normalized root-mean-square deviation of predicted vs. actual catches was calculated as the CV of the model:

$$CV_{rmsd\ S} = \frac{\sqrt{\sum_{i=1}^{n}\left(_{predicted}C(N)_{S\ day\ i} - _{actual}C(N)_{S\ day\ i}\right)^2 / n}}{mean\left(_{actual}C(N)_{S\ day\ i}\right)}$$

$$= 16.505 \times 10^6 / 11.904 \times 10^6 = 138.7\% \qquad \textbf{(A7-S)}$$

$CV_{rmsd\ S}$ was added to the variability of the GAM-predicted individual weight averages for the season (Figure A1-S); equal to a CV of 1.52% south. CVs of the depletion were then calculated as the sum:

$$CV_{depletion\ S} = \sqrt{CV_{rmsd\ S}^{\ 2} + CV_{GAM\ Wt\ S}^{\ 2}} = \sqrt{138.7\%^2 + 1.52\%^2}$$

$$= 138.7\% \qquad \textbf{(A8-S)}$$

Combined Bayesian models

For the north sub-area, joint optimization of Equations **3** and **4** resulted in parameters values:

$$_{Bayesian}N1_{N\ day\ 221} = 0.240 \times 10^9$$
$$_{Bayesian}q_N = 2.541 \times 10^{-3}\ ^{p} \qquad \textbf{(A9-N)}$$

These parameters produced the fit between predicted catches and actual catches shown in Figure A2-N.

For the south sub-area, the joint optimization of Equations **3** and **4** resulted in parameters values:

$$_{Bayesian}N1_{S\ day\ 210} = 0.941 \times 10^9; \quad _{Bayesian}N2_{S\ day\ 220} = -0.159 \times 10^9$$
$$_{Bayesian}N3_{S\ day\ 248} = 0.009 \times 10^9$$
$$_{Bayesian}q_S = 2.927 \times 10^{-3}\ ^{q} \qquad \textbf{(A9-S)}$$

These parameters produced the fit between predicted catches and actual catches shown in Figure A2-S.

[o] Off the scale but corresponding to Figure 8-left.
[p] On Figure 6-left.
[q] On Figure 8-left.

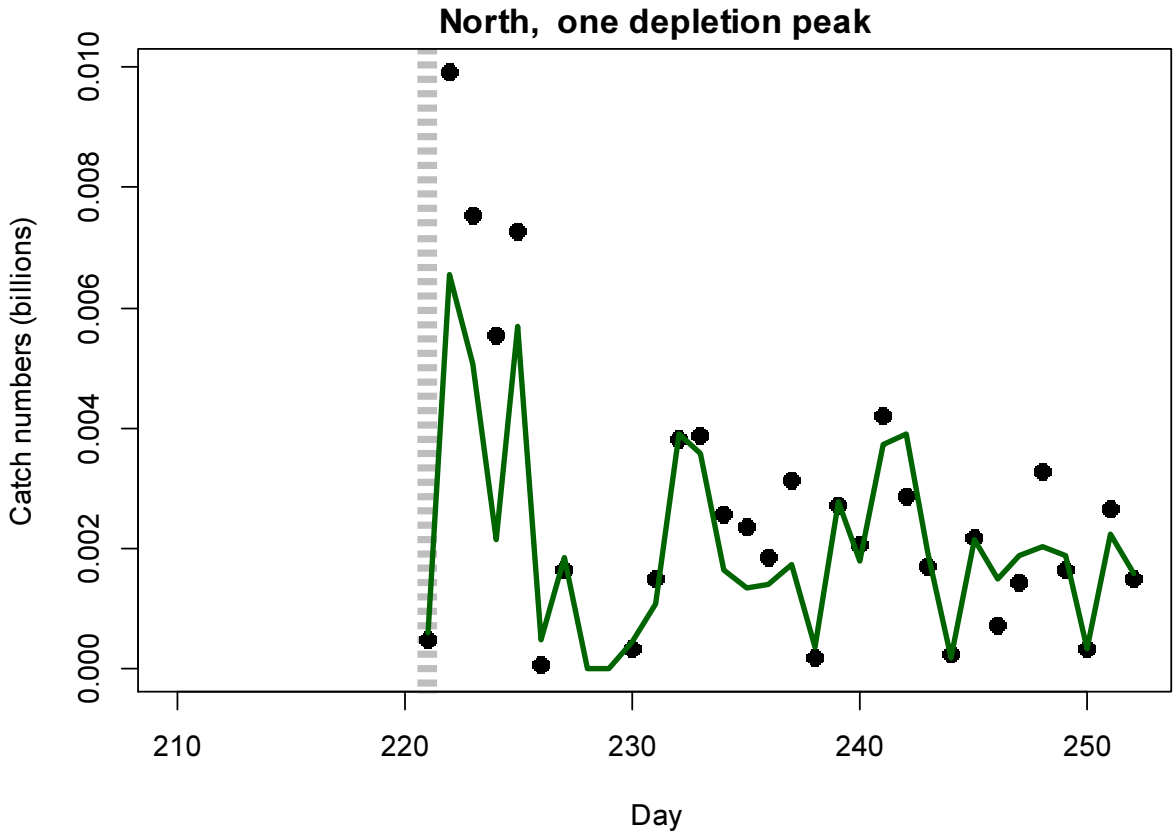
North, one depletion peak
Catch numbers (billions)
0.000
0.002
0.004
0.006
0.008
0.010
210
220
230
240
250
Day

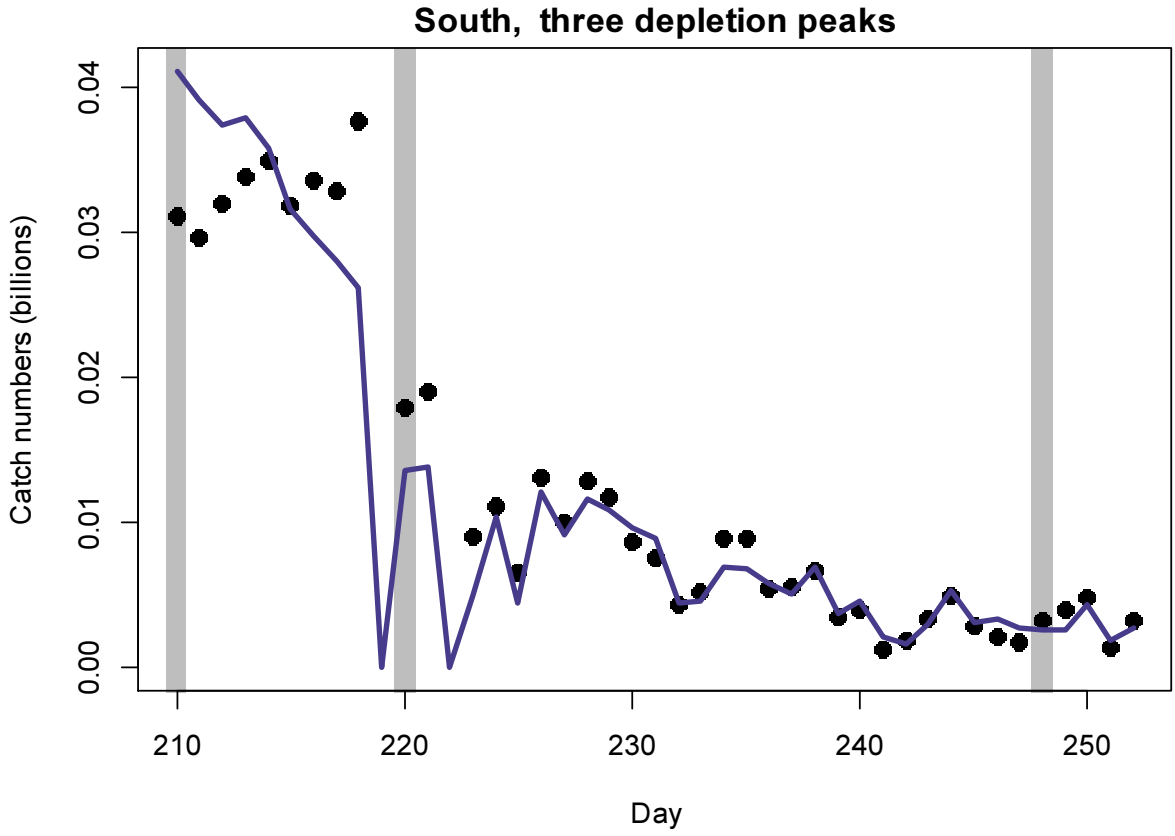
South, three depletion peaks
Catch numbers (billions)
0.00
0.01
0.02
0.03
0.04
210
220
230
240
250
Day

Figure A2-N [previous page top]. Daily catch numbers estimated from actual catch (black points) and predicted from the depletion model (green line) in the north sub-area.

Figure A2-S [previous page bottom]. Daily catch numbers estimated from actual catch (black points) and predicted from the depletion model (purple line) in the south sub-area.

Natural mortality

Natural mortality is parameterized as a constant instantaneous rate M = 0.0133 day^{-1} (Roa-Ureta and Arkhipkin 2007), based on Hoenig's (1983) log mortality vs. log maximum age regression applied to an estimated maximum age of 352 days for *Doryteuthis gahi*:

$$\log(M) = 1.44 - 0.982 \times \log(age_{max})$$

$$M = \exp(1.44 - 0.982 \times \log(352))$$

$$= 0.0133 \quad \textbf{(A10)}$$

Hoenig (1983) derived Equation **A10** from the regression of 134 stocks among 79 species of fish, molluscs, and cetaceans. Hoenig's regression obtained $R^2 = 0.82$, but a corresponding coefficient of variation (CV) was not published. An approximate CV of M was estimated by measuring the coordinates off a print of Figure 1 in Hoenig (1983) and repeating the regression. Variability of M was calculated by randomly re-sampling, with replacement, the regression coordinates 10000× and re-computing Equation **A10** for each iteration of the resample (Winter 2017a). The CV of M from the 10000 random resamples was:

$$CV_M = SD_M / Mean_M$$

$$CV_M = 0.0021 / 0.0134 = 15.46\% \quad \textbf{(A11)}$$

CV_M over the aggregate number of unassessed days between survey end and commercial season start was then added to the CV of the biomass prior estimate and the CV of variability in vessel catches on start day (Equations **A5-N** and **A5-S**). CV_M was further expressed as an absolute value and indexed by sign(1 - CV_M) to ensure that the value could not decrease if CV_M was hypothetically > 100%.

Total catch by species

Table A1: Total reported catches and discard by taxon during second season 2019 X-license fishing, and number of catch reports in which each taxon occurred. Does not include incidental catches of pinnipeds or seabirds.

Species Code	Species / Taxon	Catch Wt. (KG)	Discard Wt. (KG)	N Reports
LOL	*Doryteuthis gahi*	24748100	12434	635
HAK	*Merluccius hubbsi*	90278	3899	472
PAR	*Patagonotothen ramsayi*	77817	77777	565
BAC	*Salilota australis*	34801	2001	135
RAY	Rajiformes	17675	6264	440

MED	Medusae sp.	7550	7550	130
WHI	*Macruronus magellanicus*	7008	540	48
KIN	*Genypterus blacodes*	6624	2386	105
CGO	*Cottoperca gobio*	2995	2995	280
TOO	*Dissostichus eleginoides*	1871	1313	228
DGH	*Schroederichthys bivius*	1829	1829	212
GRV	*Macrourus* spp.	1777	1255	81
MUN	*Munida* spp.	1365	1365	82
UCH	Sea urchin	1177	1177	42
ILL	*Illex argentinus*	1122	408	87
SPN	Porifera	673	673	8
ING	*Moroteuthis ingens*	643	643	78
SCA	Scallop	502	502	40
DGX	Dogfish / Catshark	227	227	36
GRF	*Coelorhynchus fasciatus*	208	208	9
MYX	*Myxine* spp.	127	127	21
OCT	*Octopus* spp.	98	98	21
DGS	*Squalus acanthias*	91	91	28
GRC	*Macrourus carinatus*	86	32	2
BLU	*Micromesistius australis*	58	58	12
LAR	*Lampris immaculatus*	35	35	1
POR	*Lamna nasus*	35	35	1
MUL	*Eleginops maclovinus*	14	14	3
EEL	*Iluocoetes fimbriatus*	6	6	4
PTE	*Patagonotothen tessellata*	4	4	1
PAT	*Merluccius australis*	2	2	1
Total		25004798	125948	635

Trawl area coverage

Area coverage was defined as the length of trawls × their trawl door width. For each of the 1881 trawls taken during the season (Figure 2), trawl door widths were obtained from the vessels' fishing reports. Missing trawl door widths were assigned as the average for that vessel for the season. The area cover of each trawl was then calculated as the rectangle of half the trawl width on either side of the start to end positions recorded for the trawl. This calculation implies the trawl to have been linear. However, if the Euclidean (straight-line) distance between start and end position was less than 80% of the trawl's timed distance (duration × average speed), the trawl was assumed to have turned. As turns are not reported, there is no direct way to infer the true track. Instead, an extension point was optimized starting from the start point and overshooting the end point, so that the aggregate distance from the start to the extension point and from the extension point back to the end was equal to the timed distance[r].

The rectangular areas of all trawls and extension-trawls were then projected onto the Loligo Box. To estimate the areal proportion covered, the Loligo Box was discretized on a scale of 3 × 3 m. To make the amount of data points this produced tractable, the Loligo Box was further subdivided into grids of 5 × 5 km. As border grids intersected the Loligo Box, for each grid the actual number of points located within the Loligo Box (maximum (5000 ×

[r] Thus, every trawl track remained linear; going back and forth. This algorithm differs from the previous seasons' analyses (Winter 2018a, Winter 2019) in which a pivot point was optimized that could lie to some extent off the track. That has been found to give implausible deviations. It remains assumed that the start and end coordinates are accurate.

5000)/(3 × 3) = 2778889 points) was first calculated by using the 'point.in.polygon' function of R package 'sp' (Pebesma et al. 2018), both on the delineation of the Loligo Box (inclusively) and on the delineation of the Beauchêne Island Zone (exclusively). Then, any points were eliminated that corresponded to water depth of <10 m, interpolated from a GEBCO_08 30 arc-second bathymetry grid (British Oceanographic Data Centre). Finally, the grid was looped through the projection of each trawl and extension-trawl area by turn[s], and again using 'point.in.polygon', the points covered by each trawl / extension-trawl were iteratively summed. For all rectangulations and area calculations, coordinates were converted to WGS 84 projection in UTM sector 21F using R library 'rgdal' (proj.maptools.org).

Outputs derived from the calculations were the total area proportion of the Loligo Box trawled, the cumulative numbers of trawl passes over any proportion of the Loligo Box, the concentration of *D. gahi* catch by area proportion of the Loligo Box, and the concentration of effort by area proportion of the Loligo Box.

[s] In practice, to reduce computer time subsets of trawls were preselected that intersected each given grid.